Working Paper Series

Marco D'Errico, Stefano Battiston,
Tuomas Peltonen, Martin Scheicher

How does risk flow in the
credit default swap market?

No 2041 / March 2017

Abstract

We develop a framework to analyse the Credit Default Swaps (CDS) market as a network of risk transfers among counterparties. From a theoretical perspective, we introduce the notion of *flow-of-risk* and provide sufficient conditions for a *bow-tie* network architecture to endogenously emerge as a result of intermediation. This architecture shows three distinct sets of counterparties: i) Ultimate Risk Sellers (URS), ii) Dealers (indirectly connected to each other), iii) Ultimate Risk Buyers (URB). We show that the probability of widespread distress due to counterparty risk is higher in a bow-tie architecture than in more fragmented network structures. Empirically, we analyse a unique global dataset of bilateral CDS exposures on major sovereign and financial reference entities in $2011 - 2014$. We find the presence of a bow-tie network architecture consistently across both reference entities and time, and that the flow-of-risk originates from a large number of URSs (e.g. hedge funds) and ends up in a few leading URBs, most of which are non-banks (in particular asset managers). Finally, the analysis of the CDS portfolio composition of the URBs shows a high level of concentration: in particular, the top URBs often show large exposures to potentially correlated reference entities.

Keywords: flow-of-risk, systemic risk, credit default swap, financial networks, network architecture
JEL codes: G10, G15.

Non-technical summary

Over The Counter (OTC) derivatives markets represent a key channel for the propagation of direct contagion in the financial system. Interest Rate and Credit Default Swaps (CDS), for instance, account for a considerable share of banks' intra-financial exposures (in particular for the G-SIBs). Notwithstanding the rapid advancement of central clearing, the majority of trades remains on a bilateral basis: the resulting opacity and complexity in the network of exposures contribute to systemic risk as the Lehman Brothers and AIG episodes have illustrated. Although the CDS market has shown its systemic role during the global financial crisis, its structure has not yet received a lot of attention by researchers.

Since a CDS is essentially an insurance contract against the default of an underlying entity, these derivatives entail a transfer of underlying credit risk and the correspondent exposure to counterparty risk. In particular, we find that the structure of the CDS market is characterised by the existence of long chains of intermediation, where risk is passed among a set of "dealers" which comprises the set of G-SIBs and may include other market participants (e.g. hedge funds). Dealers typically run matched positions as their business model is oriented towards intermediation rather than outright risk retention. Dealers are therefore both risk buyers and sellers and generate a complex network of exposures. This series of risk transfers among market players creates a particular *flow-of-risk*, which is the main concept we analyse in this paper.

First, we formalise the notion of flow-of-risk and show that underlying and counterparty credit risk have opposite directions. We then provide sufficient conditions for a bow-tie network architecture to endogenously emerge as a result of the role dealers play in this market combined with the large amount of intra-dealer exposures. This architecture shows three distinct set of counterparties: i) a set of Ultimate Risk Sellers (URS), ii) a set of dealers indirectly exposed to each other in terms of counterparty risk, and iii) a set of Ultimate Risk Buyers (URB). We show analytically that the probability of widespread distress due to counterparty risk is higher in a bow-tie architecture than in more fragmented network structures. This is related to the role AIG and Lehman played in the CDS market at the onset of the crisis: in our framework, we identify AIG as an URB and Lehman as a dealer.

Empirically, we use a large and novel dataset to analyse counterparty risk as well as fundamental credit risk in bilateral CDS exposures network. The dataset, obtained from the DTCC, comprises virtually all gross and net exposures worldwide on 162 reference entities, including all major sovereign and financial reference entities. Our data set contains annual snapshots in the years 2011 to 2014 and it covers around 30% of the global single name CDS market. Our empirical analysis delivers three main results. First, we find that the CDS network shows precisely a bow-tie network architecture for the vast majority of reference entities across all time snapshots. Second, by identifying URSs and URBs, we are able to understand in which sectors of the economy the flow-of-risk originates and in which sectors it ends up. The flow of underlying credit risk originates from a large number of URSs and ends up in a very few leading URBs, the largest majority of which are non-banks. Third, the analysis of the CDS portfolio composition of the URBs shows a high level of concentration in the market: in particular, the top URBs often show large exposures to correlated reference entities.

1 Introduction

Over the Counter (OTC) derivatives markets provide an important channel for the propagation of contagion in the financial system (Haldane, 2009; Cont, 2010; Clerc et al., 2013; Brunnermeier et al., 2013; Benos et al., 2013). For many G-SIBs (Global Systemically Important Banks), approximately half of the value of intra-financial assets is represented by OTC derivatives (Allahrakha et al., 2015). Moreover, despite the rapid progress of central clearing, a large share of derivatives transactions continues to be conducted on a bilateral basis. The resulting opacity and complexity in the network of exposures can contribute to systemic risk (Haldane, 2009) as both the Lehman Brothers and AIG episodes have showed. The motivation for this paper stems from the multi-faceted nature of the Credit Default Swaps (CDS) market microstructure. A CDS works as an insurance contract built upon the bilateral transfer of the underlying (or "fundamental") credit risk relative to a specific reference entity (or a set of reference entities) from a *protection buyer* or *risk seller* to a *protection seller* or *risk buyer*. We use the two concepts "selling protection" and "buying risk" interchangeably. The risk arising from the default of the underlying reference entity is not the only type of credit risk involved in CDS: when a counterparty buys protection from (i.e. sells fundamental credit risk to) another counterparty, it becomes naturally exposed to *counterparty* risk, i.e. the risk that the protection seller will not honour the contract. However, the nature of the risks arising from this market is not only bilateral. In fact, it has been long known that the CDS market shows a high degree of *intermediation* and the major investment banks, while acting as dealers, do not "retain" underlying credit risk in their portfolios and tend to resell it to other market participants, therefore becoming themselves risk sellers and generating a complex network of exposures, frequently described as a "core-periphery" structure (see, e.g., Peltonen et al., 2014). The purpose of our paper is to investigate risk transfers among market participants (i.e. how underlying credit and counterparty risks are transferred) and market structure in the CDS market using network analysis tools. Our contributions are both theoretical and empirical.

From the theoretical point of view, we introduce the notion of flow-of-risk in a financial network and propose a graph-theoretical methodology to identify where the flow-of-risk originates and where it ends up. We prove sufficient conditions for the so-called bow-tie network architecture to emerge. In this architecture, underlying credit risk flows from a set of Ultimate Risk Sellers (URS), into a single set of strongly connected (i.e. forming closed chains of intermediations) Dealers, and eventually ends up into a set of Ultimate Risk Buyers (URB).

Empirically, we analyse a unique global dataset of bilateral CDS exposures on major sovereign and financial reference entities in the years 2011–2014 from the DTCC (Depository Trust & Clearing Corporation) and provide several empirical findings. First, we find that a bow-tie structure is present for almost all reference entities across time. Second, an important result of our network analysis is that the trades between the strongly connected dealers represent the majority (about $60\% - 90\%$) of traded CDS notional. Although this stylised fact was first documented by Flood (1994) and Lyons (1995, 1997) in the FX derivative market and identified as a result of so-called "hot potato" (Burnham, 1991) trades between dealers, it was not analysed in a network setting. A third general empirical finding is that the underlying credit risk flows from a high number of URSs to a small number of URBs, where ultimate risk concentrates in a few leading counterparties. Such concentration may lead to higher distress levels in the system, in case the leading URBs are exposed to correlated reference entities. Finally, we find that, for specific types of reference entities, ultimate risk is not retained within the banking system but flows into non-banking institutions, including asset managers, thereby raising concerns to what extent these institutions may be systemically important.

Major traders in the market are frequently in the middle of this series of risk transfers and hence at the centre of the flow-of-risk. These large institutions are often referred to as *dealers* and they typically maintain a matched book, i.e. their net exposures on each given reference entity are very low with respect to their total gross exposures (Stulz, 2010). Yet, these institutions are also largely exposed to counterparty risk, should any of their direct protection sellers default or be in distress. In fact, as

we will show empirically, dealers have very large exposures among themselves, thereby reflecting large counterparty risk. Indeed, it is within these intra-dealer positions where the vast majority of CDS notional traded concentrates.

However, not all large institutions have relatively low net exposures. For example, in the course of the 2007/2008 crisis, AIG was heavily involved in the CDS market. Indeed, as the International Swaps and Derivatives Association (ISDA) points out, "AIG was unique among large CDS participants in that it ran a *one way* book consisting almost entirely of *sold* protection [emphasis ours]; CDS dealers, in contrast, maintain "matched books" that balance sold with bought protection so net exposure is low."[2] In other words, AIG was acting exclusively as a buyer of risk (seller of protection). By accumulating underlying credit risk, AIG became an important source of counterparty risk. Nevertheless, AIG was not required (given its initially high credit ratings) to post collateral to its counterparties. Therefore, despite their low overall net exposures, dealers exposed to AIG would experience losses, in case of default of a reference entity, as they were still compelled to provide protection to those counterparties to whom they sold CDS. Such losses arise from pure counterparty risk: underlying credit risk is therefore transformed into counterparty risk and flows along the various chains of counterparties. This interlinked structure posed problems not only conditional upon the default of a given "risky" reference entity. In fact, when news about AIG's exposures to other stressed markets (e.g. CDOs) started to spread, the perception that AIG would be less likely to repay its obligation led to increased demand for collateral which subsequently led to a liquidity crisis that called for AIG's bailout and affected the whole financial system by generating sizeable mark-to-market losses European Central Bank (2009). In this paper, we propose a model of contagion based on this type of losses.

Lehman Brothers, on the other hand, occupied a different position in the network of CDS exposures. It had a "central position as a dealer" (Fender et al., 2008), likely to seek a matched book rather than an unbalanced net total exposure like AIG. Overall, the AIG and Lehman cases represent an example of enhanced fragility due to the counterparty network structure: Haldane (2009) argues that market participants were "fearful not so much of direct counterparty risk, but of indirect counterparty risks emanating *from elsewhere in the network*". In our *flow-of-risk* approach, AIG would have been identified as an "Ultimate Risk Buyer", exclusively exposed to underlying credit risk; in contrast, Lehman would have been identified as a "dealer", exposed to both underlying and counterparty risk. These two examples show that the network position of an institution is a key aspect in order to understand its relevance in terms of systemic risk.

Related works

Our paper is related to several strands of literature. The mechanics of intermediation is of great importance in our approach. Allen and Santomero (1997) points out that modern derivative markets tend to be "mainly markets for intermediaries rather than individuals or firms' and this is not fully reconciled within traditional theories. In this respect, some theoretical models have predicted the existence of intermediation via one or more counterparties in generic OTC markets (Amihud and Mendelson, 1980). In particular, in foreign exchange markets (FX), inventories imbalances have been proposed as the origin of the so-called "hot potato trading" (Burnham, 1991; Flood, 1994), i.e. a search process in which market participants engage in a series of *repeated passing* of positions in order to manage inventory imbalances (Lyons, 1995, 1997).[3] More recently, intermediation has been modelled in the context of CDS markets as chains of protection purchasing (Cont and Minca, 2015). Relatedly, Zhong (2014) models the formation of inter dealer networks in terms of risk sharing and the role of collateral; Hollifield et al. (2014) study the structure of the dealer network and its relation to bid-ask spreads, finding a core of central dealers

---

[2]ISDA, "AIG and Credit Default Swap", available at `http://www.isda.org/c_and_a/pdf/ISDA-AIGandCDS.pdf`. Also (European Central Bank, 2009) identifies AIG as a "one-way seller".

[3]Burnham (1991) states that a dealer "seeks to restore its own equilibrium by going to another marketmaker or the broker market for a two-way price. A game of *hot potato* has begun..."

and other peripheral ones, a result that we find also in our empirical analysis of the CDS network. Empirically, the development of chains of intermediaries (dealers) in OTC markets have been explained, for instance, by search costs (Hansch et al., 1999) and inventory management (Reiss and Werner, 1998). In the context of CDS, the role of intermediation has been analysed in Shachar (2012), who investigates how intermediation capacity and order imbalances in the CDS dealer market impact prices. Oehmke and Zawadowski (2015b) explore what determines the amount of CDS notional, finding that CDS have a standardisation and liquidity function in the market. Clerc et al. (2013) have documented that many global systemically important banks (G-SIBs) play a pivotal role in the CDS market. While these institutions tend to act primarily as dealers (and therefore have small net positions), they have large exposures to each other accounting for about 70% of the total notional traded in the market (Benos et al., 2013), and therefore are an important source of counterparty risk (European Central Bank, 2009).

Our paper relates also to other streams of literature. The application of network theory to finance and, particularly, in relation to systemic risk, has been recently receiving broad attention (see, e.g. Elliott et al., 2014; Acemoglu et al., 2015) and it now represents one of the main tools for both scholars and policymakers in the analysis of financial stability and systemic risk (Haldane, 2009). Peltonen et al. (2014) analysed and described the structure of the CDS network with a dataset similar to ours, focussing, however, on aggregated exposures. Other works, such as Duffie et al. (2015) and Cont and Minca (2015), adopt a network approach to investigate the role of central clearing. As regards counterparty risk, Arora et al. (2012) analyse pricing data from the 2008/2009 period, finding that counterparty risk is indeed priced in CDS transactions, but only to a very small extent. Another related stream of literature studies the role of intermediation, which has been investigated, e.g. by Duffie et al. (2005) who investigate how intermediation and asset prices in over-the-counter markets are affected by illiquidity associated to search and bargaining.

Paper outline

The remainder of this paper is organised as follows. In Section 2 we develop our theoretical framework, which can be divided into two parts: first, we develop a model of contagion related to how risk flows (with particular reference to the flow of counterparty risk) and show which network architectures are more conducive to contagion; second, we provide sufficient conditions for the emergence of a bow-tie network architecture in a financial network. Section 3 describes the dataset and illustrates the empirical results. Section 4 summarises the main theoretical and empirical results and concludes. Proofs of the theorems and lemmas in Section 2, alongside useful concepts on graph theory, are reported in the Appendices.

2 Flow-of-risk: theory

In this Section, we provide the main theoretical results related to our flow-of-risk approach. First, we define the network of CDS exposures and the main conventions adopted throughout the paper. In particular, we will start by defining the CDS network and introducing a distress mechanics. Second, we will derive theoretical results on the flow-of-risk. In particular, we show several theoretical implications of the so-called *bow-tie structure*, related to the empirical findings in Section 3. The concepts and definitions on graph theory we use in this Section are reported in Appendix A.1. Derivations and proofs are reported in Appendix A.2 and A.3.

2.1 Building the CDS network

Consider the set V of the n counterparties active in the CDS market and the set U of the s underlying reference entities. The index $i = 1, \ldots, n$ refers to the buyer of protection (i.e. the seller of fundamental credit risk) and the index $j = 1, \ldots, n$ refers to the seller of protection (i.e. the buyer of fundamental credit risk). Reference entities are indexed by the letter $k = 1, 2, \ldots s$. Let $x_{ijk}(t)$ be the *gross notional*

amount of protection bought by i from j on reference entity k or, alternatively, the gross notional amount of credit risk transferred from i to j.

We net each bilateral positions at the level of each specific reference entity k. This choice is motivated by the fact that most CDS's written between two counterparties are subject to so-called ISDA Master Agreements,[4] i.e. a standardised agreement which, once established, allows to include each subsequent transaction on a specific reference entity into the original agreement. As a consequence, at a given point in time, each CDS relationship between two counterparties entails only one receivable (or payable, depending on the counterparty's point of view), conditional upon the credit event of the underlying reference entity. Therefore, the *bilaterally netted exposure* matrix (which captures the netted amount for each bilateral position, i.e the amount of notional j owes to i upon the credit event relative to k) at a certain time snapshot t can be defined as follows:

$$a_{ijk}(t) = \max\left[0, x_{ijk}(t) - x_{jik}(t)\right] \tag{1}$$

Fixed a time t, we can see the CDS network as a collection of graphs $G_k = (V, E_k)$, $(k = 1, \ldots, s)$ with the same set of vertices for all reference entity and different set of edges. By fixing k, Equation 1 is therefore the weighted adjacency matrix of a collection of directed graphs.

The *aggregate* CDS network (as analysed, e.g., in Peltonen et al., 2014) can be obtained by simply summing the netted bilateral position over all reference entities:

$$a_{ij}(t) = \sum_k a_{ijk}(t). \tag{2}$$

As the three-dimensional matrix defined in Equation 1 contains only non-negative values, the aggregate bilateral exposure matrix in Equation 2 does not offset positions with opposite signs between two counterparties when these positions are written on two different reference entities (this approach is also followed in Duffie et al., 2015). This is motivated by the fact that, in general, reference entities are rather heterogeneous from a risk perspective and therefore it is more meaningful to keep, from our *flow-of-risk* analysis, the actual exposure, should a credit event on a specific entity occur. Formally, the adjacency matrix in Equation 2 can be associated to the the graph $G^{\text{aggr}} = (V, \bigcup_{k=1}^{s} E_k)$.

We can also build an exposure network at different levels of aggregations. For example, by identifying a specific sub-group $SG \subseteq U$ of reference entities, we can obtain a network *aggregated by group* of reference entities:

$$a_{ij}^{SG} = \sum_{k \in SG} a_{ijk} \tag{3}$$

We will make use of Equation 3 in Section 3 to analyse specific groups of reference entities.

2.2 Flow-of-risk and distress contagion: theoretical results

Starting from the CDS network defined in Equation 1, we can obtain theoretical results in order to understand how credit risk flows through the set of counterparties via their bilaterally netted links. Consider Figure 1, which illustrates a simple example of an intermediation chain (Cont and Minca, 2015) for a CDS on a given reference entity k:

1. Hedge Fund 1 buys protection from (sells underlying credit risk to) Dealer 1

2. Dealer 1 buys protection from (sells underlying credit risk to) Dealer 2

---

[4]ISDA Master agreements represent an important tool to mitigate counterparty risk. Netting applies to both payment nettings (in case of payments between solvable firms) and close-out netting (payments between one defaulting and one non-defaulting firm). By netting all possible payments between two counterparties, the overall notional reduces substantially and lowers potential losses in case of the default of a counterparty. See Mengle (2010) and Arora et al. (2012) for a more detailed explanation.
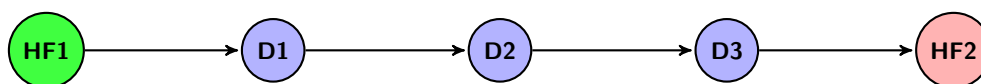
Figure 1: **Flow-of-risk**. A simple example of flow-of-risk arising from a series of bilateral transactions in CDS, involving several dealers in the intermediation process. The direction of the arrows denotes the selling of credit risk. This convention will be adopted throughout the paper.

3. Dealer 2 buys protection from (sells underlying credit risk to) Dealer 3

4. Dealer 3 (finally) buys protection (sells underlying credit risk to) from Hedge Fund 2

As a result of this intermediation chain, Hedge Fund 1 "indirectly" buys protection from Hedge Fund 2. The existence of many such chains implies that the market of CDS issued on the default of an underlying reference entity can be regarded in terms of a "flow of credit risk" (Campbell and Gallin, 2014). Such a flow is directed from market players who sell underlying credit risk to other market players who buy risk and it involves, along the way, a large number of counterparties, therefore entailing the existence of chains of counterparty risk, which constitutes the basis of the CDS network architecture.

The idea that the network architecture of CDS may be an important source of systemic risk has been put forward in the aftermath of the crisis. For example, Stulz (2010), discusses how "derivatives positions create a web of linkages across financial institutions" and discusses the "argument that this web made the financial system significantly less safe". Brunnermeier et al. (2013) focus on the systemic implications of CDS and finds several channels of contagion, including the risk originating from the network structure. In particular, Brunnermeier (2009) illustrates the "ripple effects" arising from the network structure focusing on two particular liquidity "spirals" (loss spiral and margin spiral). Zawadowski (2013) models systemic crises in an "entagled" OTC market, when counterparty risk is not fully hedged.

With our flow-of-risk approach, we aim at characterising the levels of systemic risk in the CDS markets by going beyond a mere network description of the CDS market. We will provide a formalisation of the role of each counterparty *vis-à-vis* their effective role in the spreading of distress in the network.

Large exposure to counterparty risk can be a determinant of systemic financial distress, as discussed in the Introduction. If we consider the intermediation chain reported in Figure 1, intermediaries and Hedge Fund 1 have changed the nature of their risk, *transforming* fundamental risk into counterparty risk. In general, when *both* the underlying entity and the protection seller default, then the protection buyer faces a loss, which may even trigger its default. In this light, contagion arising from the defaults of counterparties represents an evident channel of distress propagation.

However, within a mark-to-market framework, even the simple decline in the ability of repayment of an institution would imply a loss in its *direct* counteparties. For instance, the mark-to-market losses of the main counterparties of AIG were a quite substantial amount with respect to the notional value (see European Central Bank (2009) for the details). Such mark-to-market losses can then spread in the financial system, to the point of even causing the defaults of its *indirect* counterparties (Glasserman and Young, 2015). Because of these mark-to-market devaluations, even the reduction of the perceived ability of a counterparty to repay it obligations may represent a channel of contagion, especially in times of widespread financial distress.

As a matter of fact, during the financial crisis, the largest part of losses attributable to counterparty credit risk was not due to *actual defaults*, but rather to the mark-to-market loss of value conditional upon the reduction of counteparties' credit worthiness, a practice often referred to as Credit Valuation Adjustment (CVA).[5] This has practical implications since, as witnessed in the recent crisis, shocks derived

---

[5]For instance, the Basel Committee on Banking Supervision states that "roughly two-thirds of losses attributed to counterparty credit risk were due to CVA losses and only about one-third were due to actual defaults.". `http://www.bis.org/press/p110601.htm`. This figure is even higher according the loss-attribution exercise conducted by the UK Financial Service Authority (`http://www.fsa.gov.uk/pubs/discussion/dp10_04.pdf`), where reported CVA losses

from US sub-prime mortgage exposures, even though modest with respect to the balance sheet size of certain institutions, had severe consequences to the financial system via valuation losses in counterparty exposures.[6] Within a mark-to-market framework, this can trigger a sequence of devaluations down the chains of counterparties. At the onset the crisis, for instance, a large amount of outstanding value in OTC derivatives was written down because of re-evaluation of counterparty risk. However, within the Basel II framework, capital requirements focused on the variability in market values due to shifts in the underlying credit risk but no specific capital requirement was specifically aimed at addressing this type of accounting losses (Basel Committee on Banking Supervision, 2015).

Indeed, one of the crucial reforms introduced in the Basel III regulatory framework (Basel Committee on Banking Supervision, 2010) is a capital charge "for potential mark-to-market losses (i.e. credit valuation adjustment CVA risk) associated with a deterioration in the credit worthiness of a counterparty." (Basel Committee on Banking Supervision, 2010, pag. 3). Hence, mark-to-market evaluation must take into account both underlying and counterparty risk. In a CDS contract, the assessment of counterparty risk is determined by the joint event of a default of the underlying entity and the counterparty. In this Section, we develop a mechanics of distress originating from counterparty risk by taking into account both CVA and network effects. In other words, we take into account *direct and indirect* counterparty risk (Haldane, 2009).

Mark-to-market valuation We factorise the mark-to-market value of the protection leg of a CDS into the product of two factors: i) the probability of defaults of the underlying (underlying credit risk) and ii) the probability of the complement of the event of counterparty default *given* the default of the underlying (counterparty risk). Consider the notional amount of the bilateral exposure a_{ijk}, as in Equation 1 and the transpose graph $G'_k = (V, E'_k)$. We examine the value of the contract from the point of view of all the protection buyers from (risk sellers to) j, i.e. the direct counterparties of j. We denote this set as N_j, which represents, in network terms, the set of the neighbors of j. When k does not default, then the CDS pays zero, regardless of the default of j. When k defaults, two scenarios may occur.

If counterparty j does not default, then i receives the full notional less the settlement (either physical or in cash), i.e. $a_{ijk}(1 - \rho_k)$, where ρ_k is the recovery rate on the obligations of k. If j defaults, then i recovers a fraction dependent on both ρ_k and ρ_j (the recovery rate of j). We can therefore write the market value of the obligation for all $i \in N_i$ as the expected value M_{ijk} (see Appendix A.3 for the derivation) of the payoff of the protection leg of the contract:

$$M_{ijk} = a_{ijk} \underbrace{p(k)\,(1 - \rho_k)}_{\text{underlying credit risk}} \underbrace{(1 - (1 - \rho_j)p(j|k))}_{\text{counterparty risk}}, \quad \forall i \in N_j. \tag{4}$$

In Equation 4 we can see the role of the probability of default for the underlying entity. In this formula, we consider the conditional probability $p(j|k)$ without assuming a specific dependence structure between the default events of k and j. The term $p(j|k)$ captures an important aspect of a CDS contract, i.e. that counterparty default matters in the valuation of the contingent claim *conditional* to the default of the underlying. All the direct counterparties in the set N_j would be affected by an increase in this conditional probability.

Equation 4 also shows that the mark-to-market value is proportionally increasing w.r.t. the probability of default of the underlying. In case the default of j and k were highly correlated event, $p(i|k) = p(j,k)/p(k) \to 1$ as either $p(j)$ or $p(k)$ increase. In general, since $p(j|k) = p(k|j)\frac{p(j)}{p(k)}$, then M_{ijk} decreases

---

are about five times as large as losses from defaults. See also the European Banking Authority report on CVA (https://www.eba.europa.eu/documents/10180/950548/EBA+Report+on+CVA.pdf).

[6]A growing body of work has dealt with problems arising from mark-to-market evaluation, with particular reference to widespread systemic losses even in the presence of relatively small initial shocks (see, for instance, Adrian et al. (2008); Plantin et al. (2008); Castrén and Kavonius (2009); Battiston et al. (2016a,b)). Visentin et al. (2016) provide a common framework to compare different contagion models, highlighting the role of claim valuation in a networked financial systemic, which is explicitly formalised in Barucca et al. (2016).

with respect to the increase of $p(j)$. Any shock (either originating from outside the network or within the network) which implies an increase in $p(j)$, would *reduce* the mark-to-market value of the obligation of any counterparty in the neighbour set N_j.

In order to better highlight the negative dependence on $p(j)$, we show, for illustrative purpose, how Equation 4 can simplify in the case of i) zero recovery rates ($\rho_k = \rho_j = 0$, a reasonable assumption at least in the very short run), and ii) *independence* of the default events of i and j. Under these assumptions, we can write the market value in Equation 4 as follows:

$$M_{ijk}^{\text{ind}} = a_{ijk}\, p(k)\, (1 - p(j|k)) = a_{ijk}\, p(k) \left(1 - \frac{p(j)p(k)}{p(k)}\right) = a_{ijk}\, p(k)\, (1 - p(j)), \quad \forall i \in N_j. \qquad (5)$$

From Equations 5 it is immediate to notice the negative dependence of the mark-to-market valuation with respect to the probability of default of the counteparty j: should $p(j)$ increase, then the mark-to-market value of the obligation would decrease and all the counterparties $i \in N_j$ would experience a mark-to-market loss on their asset side.

An important remark is place. The distress process we introduce aims at capturing the fact that, in a CDS network, underlyingcredit risk may become counterparty risk. However, the order of magnitude of the counterparty risk associated may be lower with respect to the underlying notional amount, and will depend on several elements including the presence of collateral (both at the level of initial and variation margins) and buffers built up for losses as the reference entity's risk increases or decreases. In the case of "jump to default" of the underlying entity, a CDS contract entails a sudden payment from the protection seller. These buffers are the key element of the "standardised approach" for counterparty risk exposures as proposed by the Basel Committee on Banking Supervision.[7]

Therefore, estimating the amount of such risk crucially depends on data availability, which ideally would include the amount of underlying credit risk being hedged via bond holding (or other derivatives) and the amount of collateral accrued via initial and variation margins. These data are becoming increasingly more available to regulators and policymakers (Abad et al., 2016). Our approach represents the starting point for identifying institutions that can represent sources of risk and understanding how risks can propagate throughout the network.

Distress mechanics   We consider a multi-period model, with time indexes $t = 0, 1, 2, \dots$. At $t = 0$, we observe the initial CDS network configuration; all counterparties have allocated their CDS exposures. In this work, we do not explicitly model the process of network formation. Rather, we consider the CDS network at $t = 0$ as the result of an implicit optimal allocation strategy the individual agents in the network, which allows us to comparison different network structures in terms of how distress propagates in the system. In fact, the literature on financial network has shown that, while there are benefits from interconnectedness (e.g. increased diversification, trading opportunities, enhanced market liquidity), a highly densely interconnected financial system may also result in more fragile structures (Acemoglu et al., 2015), especially in the case of large enough shocks (Glasserman and Young, 2015). For ease of notation, we fix a reference entity and drop the index k: the network of underlying credit risk transfers is represented by the graph $G = (V, E)$.

At $t = 1$, a subset of counterparties $C_1 \in V$ faces an initial distress, defined as a loss on their asset side. Given the complexity of the network of CDS exposures, the flow-of-risk could present a number of different patterns: the network could indeed present different architectures, with very complex structures. We therefore develop a general mechanism of distress, which can be applied to any kind of network architecture. The fundamental mechanics of the model is as follows: a loss in the asset side of a counterpaty j produces, *ceteris paribus*, a reduction of j's equity, therefore decreasing $j's$ *distance to default* (Crosbie and Bohn, 2003). Since j will be less likely to repay its obligation (as in the classic Merton, 1974, approach), this translates into an increase of $p(j)$. The assumption of unaltered financial conditions

---

[7]See http://www.bis.org/publ/bcbs279.pdf

and, in particular, assuming no potential positive cashflow, reflects a setting when a widespread financial crisis rapidly affects the system (e.g., a general loss of confidence or widespread panic in the market) and financial institutions cannot quickly react by raising enough capital to offsets their mark-to-market losses and maintain their original credit worthiness. In this case, the mark-to-market value of any type of obligations owed by the direct counterparties (i.e. forall $i \in N_j$) will reduce as well, thereby causing a loss in all the counterparties of j. At this point, under the same assumption, the distress will then proceed further in the network.

Our distress model, hence, is meant to capture distress contagion that spreads in the network even before the actual default of a counterparty. This approach is consistent, for instance, with previous work on financial integration (Stiglitz, 2010), models on interbank distress (Battiston et al., 2012, 2016a; Barucca et al., 2016) and the qualitative description provided by Stulz (2010) (who specifically refers to the CDS market). Moreover, it models how distress originating from counterparty risk spreads in a CVA framework. Formally, we model this mechanism by assuming that the *conditional* probability that a node is in distress given that any of its direct counterparties is in distress is one:

$$P\left(i \in C_{t+1} | (j \in C_t, i \in N_j)\right) = 1 \tag{6}$$

The dynamics in Equation 6 identifies a set of distressed nodes C_t at each time t, conditional upon the set of distressed nodes at $t-1$. With such mechanics at play, we can determine how the initial distress from any $j \in C_1$ (i.e. the set of initially distressed nodes) propagates in the network. The process continues iteratively until a certain time T, where all counterparties are either distressed or not.

One of the key graph-theoretical concepts we use in the model is that of *reachability* (see Appendix A.1). We say that, given the transpose CDS graph G', the reachability set of a node j is composed of all the nodes i for which there exists a path $j \to i$; in other words, the reachability set of j is composed of all its direct and indirect counterparties. The reachability set has a recursive nature, i.e. it can be expressed as the set N_j of direct counterparties of j and the union of the rechability sets of all $i \in N_j$ (see Equation 10 in Appendix A.1). The recursiveness of the reachability set in a financial network is identified in Haldane (2009) as a key feature leading to uncertainty and instability. Coupling this property with Equation 6, it follows that if a node is originally in distress, then there exists a time $t^*_{C_1}$, where all nodes in the reachability set of $\forall j \in C_1$ will also be distressed:

$$P(i \in C_{t^*_{C_1}} \mid (j \in C_1, i \in R_j)) = 1.$$

Notice that $t^*_{C_1}$ is dependent on C_1 and equal to the maximal distance between the $i \in C_1$ (i.e. where the shock has initially originated) and any node in the reachability set of C_1. Finally, we can identify the set of distressed nodes at $T = \max_{j}\{t^*_j, j \in C_1\}$ as the set of initially distressed nodes C_1 and the union set of the nodes reachable from any node in C_1:[8]

$$C_T = C_1 \cup \bigcup_{j \in C_1} R_j$$

and therefore the number of distressed nodes at T is equal to:

$$|C_T| = \left| C_1 \cup \bigcup_{j \in C_1} R_j \right| \tag{7}$$

From Equation 7, it is immediate to prove that $|C_T| \geq |C_1|$. In other words, the network structure *amplifies* the number of distressed nodes by a factor $|C_T|/|C_1|$.

---

[8] In this sense, the concept of reachability set is the graph-theoretical analogous of the notion of *risk orbit* in Eisenberg and Noe (2001).

An important results concerns the relationship with the diameter of the network. Since each $t_{C_1}^*$ is equal to the maximal distance between $j \in C_1$ and any node in its reachability set R_j, there will be at least one j such that the maximal distance indeed coincides with the diameter. In other words, the end-time T is always *bounded* by the diameter of the graph. The diameter is a global network measure which can be interpreted as a measure of vulnerability of the whole financial system with respect to the distress of any of its component. Moreover, financial systems with a low diameter may potentially give the regulator less time for intervention, including requests for additional capital buffers in a particular set of nodes.[9]

Last, we define the probability of a *systemic event* as the probability that, for a given CDS network G and conditional to a specific distress configuration C_1 at $t = 0$, at least a certain fraction ν of nodes will be in distress at $t = T$:

$$P_G^{\text{syst}} = P\left(\frac{|C_T|}{n} \geq \phi \mid C_1\right).$$

The fraction $\phi \in [0, 1]$ can be chosen in a convenient range. However, for the theorems related to systemic distress in the the next Section, we do not need to explicitly specify a value for ϕ.

To summarise, we prove two important results on the level of distress and the time it takes to reach such levels. In particular:

1. the time T at which the distress process ends is always lower or equal than the diameter of the CDS network;

2. the set of the counterparties distressed at time T is given by:

$$C_T = C_0 \cup \bigcup_{j \in C_1} R_j$$

Further, the reachability set R_j has a straighforward economic interpretation. In fact, it represents the set of those counterparties that have to reassess, *ceteris paribus*, the market value of their asset, conditional upon a loss originating in j. This straightforward financial interpretation, coupled with Equation 8 leads to one of the key results of our distress model: fundamental risk transfers between counterparties that are not directly connected generates flows of counterparty distress. Moreover, the time (and therefore the "speed") in which the distress process propagates in the network, is bounded by the diameter of the network. Indeed, the lower the diameter, the lower the upper bound for the time required for the distress to propagate in the network. The diameter of the CDS network can be interpreted as the length (meant as the number of counterparties) belonging the longest intermediation chain in the market.

2.3 Network architecture dominance

These results, although provided in the most general case, show a clear dependence on the specific network architecture. We naturally classify the counterparties into three disjoint categories: i) only risk sellers, set S, ii) only risk buyers, set B and iii) dealers, set D, who both sell and buy risk, acting as intermediaries. As we will show, the intermediation structure has a key role in determining the level of system risk implied by each specific network architecture. Within this classification, several different network architectures can arise.

Figure 2 shows three network architectures. Green nodes belong to the set S of only sellers, red nodes belong to the set B of only buyers and, last, blue nodes belong to the set D of dealers, in the middle of the intermediation chain. The three network architectures can be described as follows:

1. Figure 2a shows an architecture of intermediation where chains are *independent* from one another;

---

[9]Acemoglu et al. (2015) propose a related idea by introducing the concept of harmonic distance between two financial institutions, borrowing the concept of *mean hitting time* from Markov chain theory.

(a) Independent chains (with dealers).

(b) Interdependent chains (with weakly connected dealers).

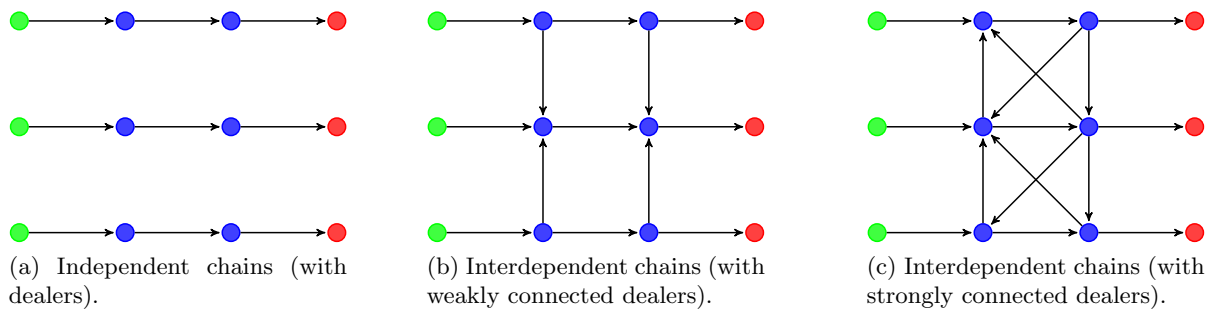(c) Interdependent chains (with strongly connected dealers).

Figure 2: Different types of intermediation structures. The direction of the arrow denotes the transfer of underlying credit risk.

2. Figure 2b shows an architecture where chains are *interdependent*, but the sub-network composed of the nodes in the set D of dealers is *not* strongly connected, i.e. they are not connected (either directly or indirectly) to all other nodes in D,

3. Figure 2c shows an architecture where chains are again *interdependent* but, in addition, the sub-network composed of the nodes in the set D of dealers is strongly connected, i.e. they are connected (either directly or indirectly) to all other nodes in D. We shall refer to this network structure as a *bow-tie*.

By using the distress process outlined above, we can prove (See Theorem 1 in Appendix A.2) that the *bow-tie* structure is the type of network with the maximal probability of a systemic event and *dominates* the other ones, as stated in the following theorem.

THEOREM 1 (Network architecture dominance)**.** *The probability of a systemic event in a bow-tie is always higher than in the case of: i) independent intermediation chains and ii) interdependent weakly connected intermediation chains. Formally:*

$$P_{ind}^{syst} \leq P_{weak}^{syst} \leq P_{bowtie}^{syst}.$$

This theorem has a key implication in terms of the way distress may propagate in the system: in a bow-tie architecture, a shock originating from just *one* node (in the only-risk buyer set) affects all the set D and all the set S. This finding is reported and proved in Theorem 2. This implies that, in a bow-tie architecture, the probability of a system-wide event is larger than in the case of a more fragmented market structure with possibly independent chains. This has particular importance especially if, *ex ante*, the structure of the market is unknown. Indeed, by assuming a fragmented market, we would underestimate the total systemic losses, conditional upon a single counterparty incurring in a loss.

THEOREM 2 (Systemic distress)**.** *Given a CDS network with a bow-tie structure then:*

- *A loss in an URB implies loss in all dealers and all URSs*
- *A loss in a dealer implies losses for all dealers and all URSs*

This theorem has an important implication related to the Lehman and AIG cases. The situation of *both* Lehman and AIG put the financial system under severe distress as all counterparties down the chain were potentially affected by the distress originating from upstream. In our empirical analysis (Section 3), we find that a very few URBs concentrate the vast majority of notional. Indeed, by using Equation 4, we can see that when ultimate risk is concentrated in the system, the distress originating from a small number of counterparty can affect the vast majority of the financial system.
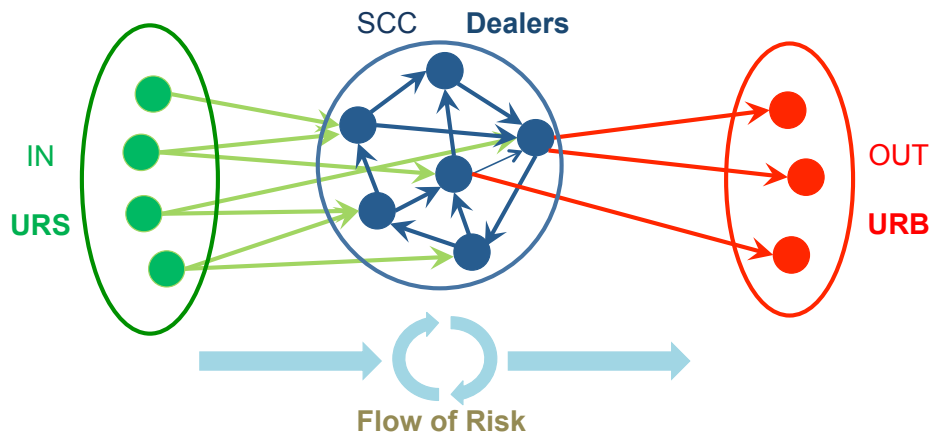
Figure 3: **Bow-tie structure and flow-of-risk**. Stylised representation of the bow-tie structure in the CDS market: risk flows from the IN component (the URS) to the SCC set (dealers) and eventually ends up in the OUT component (the URB).

2.4 The bow-tie network architecture

Bow-tie network architectures have been long known in other research fields.[10] To our knowledge, our paper is the first to make use of this notion within the context of the OTC derivatives network. First, a very important remark is in place: not every network features a bow-tie structure, therefore making network exhibiting such behaviour particularly interesting. Since the bow-tie architecture is the most critical in terms of systemic-wide distress, two natural questions arise:

1. what are the theoretical conditions for such architecture to emerge endogenously?

2. how often do we observe the bow-tie architecture in the global CDS network?

A bow-tie network is composed of the following components:

1. one and only one Strongly Connected Component (SCC), i.e. a component where from each node it is possible to find a path arriving at every other node;

2. an IN component, i.e. a unique set of nodes whose links point *only* to the SCC;

3. an OUT component, i.e. a unique set of nodes receiving links stemming only from the SCC.

Formally, if the CDS network features a bow-tie network architecture for a fixed reference entity k, then we can permute the rows and column of the matrix a_{ijk}, such that the matrix can be expressed in the following block-form (definition 1 in A.1):

$$a'_{ijk} = \begin{bmatrix} 0 & A_{\text{URS, dealers}} & 0 \\ 0 & A_{\text{dealers, dealers}} & A_{\text{dealers, URB}} \\ 0 & 0 & 0 \end{bmatrix}. \tag{8}$$

It is clear from the permuted exposures matrix reported in Equation 8 that, since this is a very specific block-matrix, not all networks present, in general, a bow-tie structure. Figure 3 depicts a stylised representation of a bow-tie network architecture as expressed in Equation 11. On the left, the IN component

---

[10]For instance, (Broder et al., 2000) find a bow-tie architecture in the World Wide Web; (Vitali et al., 2011) observe that the trans-national network of corporate ownership presents a bow-tie architecture. Krackhardt and Hanson (1993) discusses the properties of a bow-tie network architecture in the context of business relationship networks.

coincides with the set of Ultimate Risk Sellers (URS), or the institutions that stand at the very beginning of the flow-of-risk. The middle part (in blue) represents the set of intermediaries (the major dealers belong to this group), whose subnetwork of exposures is *strongly connected*.

2.4.1 Emergence of a bow-tie in an OTC network

We describe a random graph model for a general OTC network in which, under certain minimal assumptions, a bow-tie structure emerges with high probability. Consider the partitions of the set of counterparties V into disjoint sets S, B, D ($V = \{S \cup C \cup B\}$) we have proposed above. We prove that the emergence of a bow-tie structure is due to two main features of the network:

1. the presence of intermediaries (the dealers, who buy *and* sell risk at the same time),

2. a sufficient number of linkages between the set of dealers, the number of which is a non-decreasing function of the levels of "hot potato" trades.

The main result is given by the following theorem:

THEOREM 3 (Emergence of a bow-tie). *If a graph $G = (V, E)$ is such that the set of nodes can be partitioned in three disjoint subsets B, S, D and:*

A1 $\forall i \in S$ *have only out-going edges,* $\forall i \in B$ *have only in-coming edges and* $\forall i \in D$, *have at least one in-coming edge and at least one out-going edge from and to another node in D,*

A2 *the density of the graph δ is larger than a specific threshold,*

$$m > (n-1)log(n) \text{ as } n \to \infty.$$

then G has a bow-tie architecture.

Though the result holds for $n \to \infty$, if n is large enough (as in the binomial/Poisson approximation), we obtain a very good boundary condition for the emergence of a bow-tie. Two main comments are in place. The first relates to the emergence of a bow-tie architecture as the results of very minimal assumptions on the behaviour of the counterparties in the CDS market. In fact, the presence of a large enough subset of dealers, with a set D of 50 nodes, we would need only 84 bilateral exposures in order to obtain a bow-tie with very high probability. This implies a very low density of about 3.5 percent in the network. The second comment is related to the hot potato trades. These trades can either establish new links between counterparties or increase the weight of already existing links. In either cases, the number of links is a non-decreasing function of the amount of "hot potato" in the system. Remark 1 in Appendix A.3 shows that, indeed, in case of matched books with end-users, the notional levels of hot potato can be *arbitrarily large*.

Identifying a bow-tie architecture allows for the identification of what type of risk each counterparty bears in the CDS network. URS are only exposed to counterparty risk, dealers are exposed to both counterparty and fundamental risk and, last, URB are exposed only to fundamental risk. Dealers, in particular, are exposed to fundamental risk in the amount their book is unmatched.

The relevance of the theoretical findings reported in this Section will be further clarified in the next Section: indeed we will show that the bow-tie architecture can be found consistently both along the vast majority of reference entities and across time.

3 Flow-of-risk: empirical results

In this Section, we describe the main empirical results obtained by applying our flow-or-risk to a global dataset on CDS exposures. We start by describing the dataset, providing some key statistics. We then
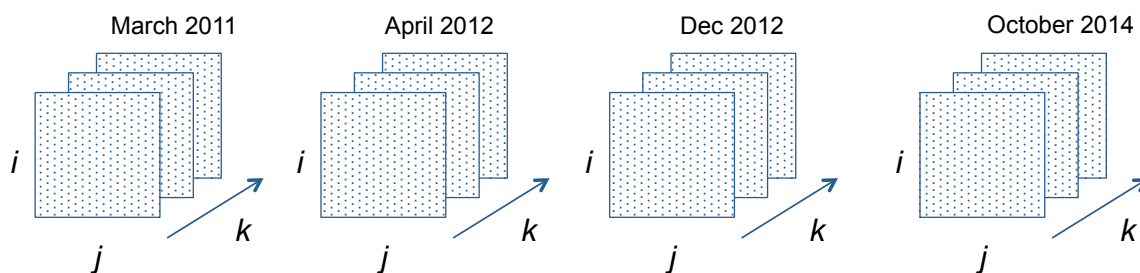
Figure 4: **Data structure**: netted bilateral exposures. The structure of our dataset. Counterparties are indexed with the letters i and j whereas the reference entities are indexed by k.

proceed analysing the presence of the bow-tie structure across reference entities and along different time snapshots. Further, we provide a detailed analysis of the portfolio composition of the different Ultimate Risk Buyers.

3.1 Data description

The dataset on CDS exposures is provided by the Depository Trust and Clearing Corporation (DTCC) and is extracted from their Trade Information Warehouse (TIW). The sample contains data from four snapshots on gross and net bilateral exposures (bilateral net exposures may be the result of several separate transactions) from 900 counterparties on around 600 major sovereign and financial reference entities. The dates of the snapshots are month-ends of March 2011, April 2012, December 2012 and October 2014. To keep the four snapshots comparable, while still retaining the largest part of the notional traded, we exclude minor counterparties active only on one or very few reference entities. We select 435 active counterparties on the most traded 162 reference entities.

Counterparties Due to the confidentiality of the data, counterparties are anonymised, but categorised in seven sectors: "asset manager", "bank", "financial services", "hedge fund", "insurance", "non financial" and "pension plan". The anonymisation of each individual counterparty is consistent across all reference entities and across the four snapshots.

Reference entities Reference entities are not anonymised and include all traded G20 sovereigns (including all traded EU sovereigns), emerging markets sovereign and several global financials, representing about one-third of the single name CDS market in terms of gross notional.[11] Our data do not include index CDSs. Last, in order to proceed with a more aggregated analysis, we divide the reference entities into eight main categories: *EU Periphery sovereigns*, *EU Core sovereigns*, *Other developed markets sovereigns*, *Emerging markets sovereigns*, *G-SIBS'*, *Bank-periphery*, *Other financials*, and *Major Bank non G-SIBs*.

The data structure is represented in Figure 4, where we "stack" the netted bilateral exposure matrices from counterparty i to counterparty j on reference entity k at each snapshot t, as in Equation 1. Table 1 reports the total (bilaterally) netted notional for the aggregated network and for each reference entity category. First, we observe a decline in notional between the first and last snapshot of roughly 30%. This can be due to several reasons, including a general decline in notional traded or the increase of

---

[11] The total gross notional of our dataset is 5.41, 5.81, 5.48, 4.02 trillion for the dates March 2011, April 2012, December 2012, October 2014 respectively. We compare these figures with the total gross notional from the BIS seminannual OTC derivatives statistics for credit default swaps (`http://www.bis.org/statistics/derstats.htm`). We find that our data cover about between one fifth and one fourth of the total market for CDS between 2011 and 2014, and one third of the single-name market.

Table 1: Total (bilaterally) netted notional (first row) disaggregated (percentage values) by each reference entity category.

	Mar 11	Apr 12	Dec 12	Oct 14
EU Periphery sovereigns	13.90%	10.85%	12.36%	14.61%
EU Core sovereigns	10.50%	12.03%	12.04%	12.99%
Other developed markets sovereigns	9.07%	10.75%	10.89%	10.80%
Emerging markets sovereigns	10.78%	11.35%	12.16%	16.18%
G-SIBS	15.07%	15.69%	14.91%	14.39%
Bank-periphery	6.13%	5.80%	5.71%	5.17%
Other financials	28.38%	27.69%	26.44%	21.11%
Major Bank non G-SIBs	6.17%	5.83%	5.48%	4.75%
Total (USD trillion)	1.221	1.222	1.107	0.869

Table 2: Total (bilaterally) netted links (first row) disaggregated (absolute values) by each reference entity category.

	Mar 11	Apr 12	Dec 12	Oct 14
EU Periphery sovereigns	2121	1806	1706	1361
EU Core sovereigns	1590	1968	1733	1443
Other developed markets sovereigns	2444	2561	2387	1901
Emerging markets sovereigns	2520	2547	2580	2260
G-SIBS	5443	5783	5282	4060
Bank-periphery	2705	2713	2552	1983
Other financials	14211	14094	13023	9094
Major Bank non G-SIBs	3344	3345	2958	2059
Total number of links	34378	34817	32221	24161

risk-mitigation techniques such as central clearing or *compression* trades, a practice aimed at reducing the total notional value traded while retaining net individual positions (Benos et al., 2013; D'Errico and Roukny, 2016). The largest part of notional is traded on EU sovereigns (and, in particular, on EU periphery sovereigns). CDS traded on G-SIBS, which could also be aimed at hedging counterparty risk, also account for a significant part of the total notional. The evolution in time of the relative notional values are also of interest. For example, we observe a sharp drop between March 2011 and April 2012 for the category "EU periphery", whereas trades on other sovereigns increased. The relative notional traded on G-SIBS is stable over time. The relative notional traded on sovereigns issued by emerging market economies and on other sovereign, instead, rises sharply in time. This rise is compensated by the decline on "Bank-periphery", major "non-dealer" and "other financials" categories. In other words, we observe a shift in notional traded from financial to sovereign reference entities.

Table 2 provides a brief overview on the statistics on the bilateral links. We observe a distinct decline in the overall number of links both in aggregate and in each individual category. This can be due to several reasons, including the general decrease in notional, the increase of compression trades (reducing the number of bilateral exposures).

3.2 Bow-tie architecture: empirical evidence

As discussed in Section 2, finding a bow-tie structure in a network of CDS has important theoretical implication in terms of how financial distress may spread in the system. We also provided sufficient conditions, based on the amount of notional traded within the set of dealers, much of which may be
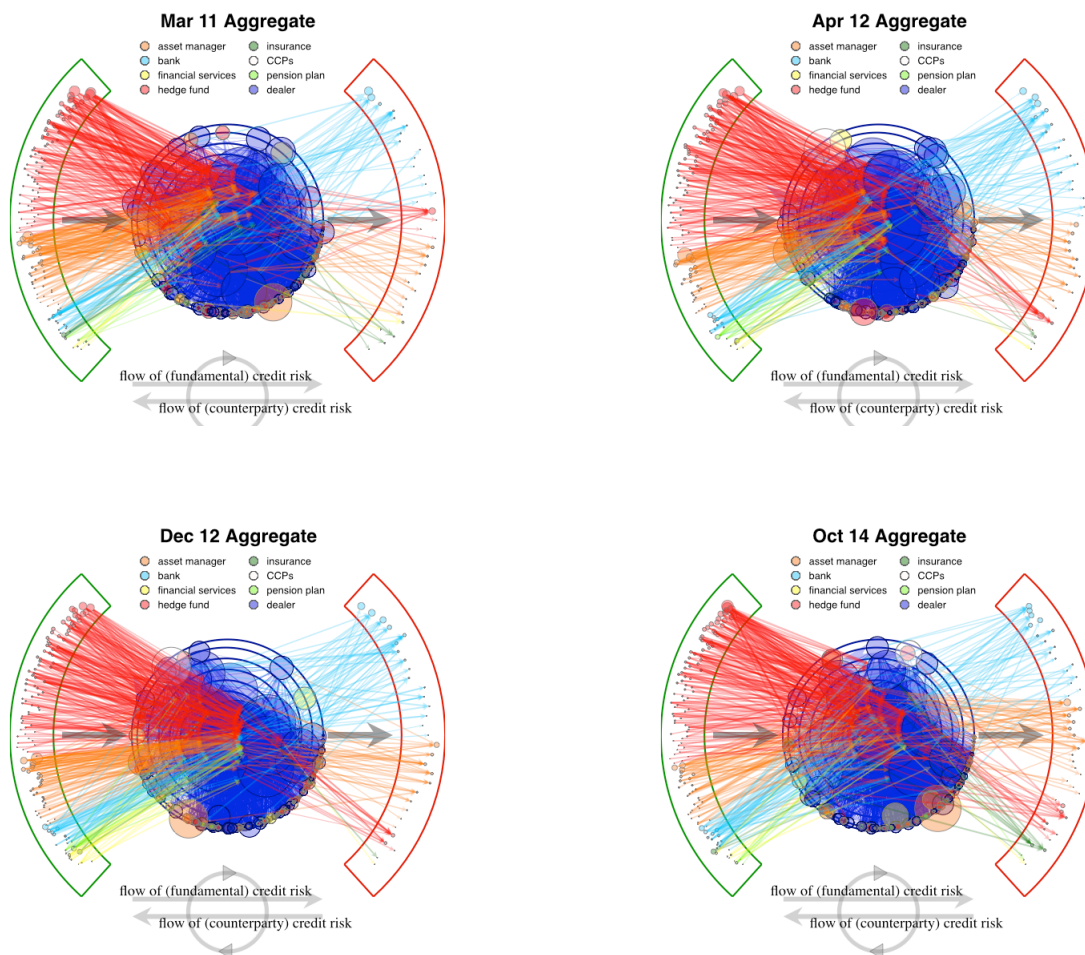
Figure 5: CDS network visualisations (aggregate network) for the four snapshots. Ultimate Risk Sellers (URS) and Ultimate Risk Buyers (URB) are ordered from the top to the bottom by notional traded at first by each sector and then within the sector.

due to "hot potato" trades. Largely confirming this theoretical prediction, our empirical analysis shows that a bow-tie architecture is present both along the vast majority of reference entities and across time snapshots.

We start by observing a bow-tie structure in the aggregate network. To this end, we analysed, at first, the aggregate CDS network in time. Figure 5 presents the aggregate networks for the four time snapshots, where we have visualised the bow-tie structure, separating the three sets of counterparties: URS, dealers and URB. In order to highlight the flow-of-risk, following the convention in Section 2, we placed the URS on the right-hand side, the strongly connected subset of dealers in the middle and the URBs on the left-hand side. The bow-tie block structure, and therefore the role of each counterparty in the flow-of-risk, is identified with the algorithm reported in Appendix A.1.2. The size of the nodes reflects the absolute gross notional traded, normalised by the maximum individual gross notional within the respective component. This implies that larger nodes in the set of URBs and URS do not necessarily trade more notional than node of the same size in the dealers' set. The nodes in the strongly connected component are placed closer to the center according to their Katz centrality (Katz, 1953), a measure that roughly captures the direct and indirect level of intermediation of a node (Friedkin, 1991).

Notice that the fact that we observe a bow-tie in the aggregate network does not naturally imply that we find a bow-tie on all reference entities or in each snapshot. In fact, given the high levels of notional traded on very few reference entities, the structure of the aggregate network can be mostly driven by these major

Table 3: **Persistence of the bow-tie structure**. For each time period, we report the median number of nodes of each component (dealers, URS, and URB) in the bow-tie (computed over the individual reference entities belonging to each subgroup of reference entities in the first column).

	Mar 11			Apr 12		
Ref entity	# dealers	# URS	# URB	# dealers	# URS	# URB
EU Periphery sovs	38.0	37.5	23.0	33.5	35.0	18.0
EU Core sovs	29.5	36.5	18.0	32.0	37.5	23.5
Other developed markets sovs	24.0	12.0	8.0	25.0	15.0	8.0
Emerging markets sovs	38.0	40.0	15.0	39.0	35.0	12.0
G-SIBs	43.0	32.0	19.0	43.0	29.0	25.0
Bank-periphery	27.5	16.0	10.5	27.5	16.0	8.0
Other financials	23.0	11.0	4.0	22.0	9.0	6.0
Major Bank-non G-SIBs	22.0	12.0	7.5	22.0	10.5	8.0
	Dec 12			Oct 14		
Ref entity	# dealers	# URS	# URB	# dealers	# URS	# URB
EU Periphery sovs	34.5	29.5	16.5	28.0	17.5	13.0
EU Core sovs	31.0	28.0	19.5	29.0	17.0	15.0
Other developed markets sovs	23.0	11.0	9.0	21.0	7.0	6.0
Emerging markets sovs	39.0	42.0	15.0	37.0	41.0	16.0
G-SIBs	44.0	23.0	24.0	35.0	19.0	23.0
Bank-periphery	25.0	13.0	7.0	21.0	11.0	6.5
Other financials	22.0	9.0	5.0	17.0	6.0	5.0
Major Bank-non G-SIBs	20.0	8.0	7.0	17.0	6.0	8.0

reference entities. We therefore analysed the network for each reference entity for each snapshot across time: we find clear-cut evidence that the CDS network consistently presents a bow-tie architecture both along the space of the reference entities and along each time snapshot. Table 3 shows the results aggregated by groups of reference entity: median values for each component within the subgroups of reference entities are reported. For example, a value of 27.50 in the dealers' set for the subgroup "Bank-periphery" reports the median size of the dealers' set for the disaggregated network referring to all reference entities belonging to that subgroup.

By analysing Table 3, we find several empirical results. First, we observe only one strongly connected component in the network for each reference entity, with exceptions for two reference entities with very low volumes in the snapshots December 12 and October 14, where, in line with our theoretical findings, bilateral trades do not give rise to the bow-tie structure. The presence of only one strongly connected component is consistent across the space of reference entities and across time. Second, we observe that the number of dealers (the nodes within the largest strongly connected component) is consistently higher than the number of URSs and URBs, hence showing the high level of intermediation present in the CDS market. Third, the number of URBs is consistently lower than the number of URSs. Therefore, we can view the URBs as the bottlenecks of the flow-of-risk. These results imply that ultimate risk is concentrated within fewer actors (see Tables 3 and 6): the analysis of the concentration of positions in the next part, will further develop these concepts.

The strongly connected component, i.e. the subnetwork induced by the set of dealers, also presents interesting characteristics. First, a very large number of financial institutions lies in this component. In particular, we observe between 13-16 major players in each reference entity trading roughly $80-90\%$ of the

notional within the SCC, while keeping a relatively low net position (i.e. "matched" books). Such large volumes point to the possibility that these large players are G-SIBs. However, given the anonymisation of our dataset, we cannot confirm this claim. These institutions are not only *strongly* connected (in the sense that there exists a path of risk transfers from and to any possible pair of the subset), but very densely connected: in fact, on the major reference entities, we observe all the possible bilateral exposures, i.e. a *fully connected* network. Second, we find a number of minor counterparties in the SCC that act as dealers on a much lesser amount of notional $10 - 20\%$. This two-tiered network structure of the dealers' subnetwork is in line with previous work on the structure of the dealer networks in the market for municipal bond (Li and Schürhoff, 2014). We confirm analogous results for the CDS dealer network. Third, an important interpretation of the fact that we observe a strongly connected component is that the mark-to-market losses induced by the distress of a counterparty can potentially reach *every* other node in the SCC. Importantly, the presence of non-banking institution in this highly interconnected core shows that also these institutions, often not regulated, might be crucial in the propagation of distress.

The fourth main result relates to notional exposures resulting from "hot potato" trades. In fact, with our methodology, we can distinguish between the notional traded by ultimate counterparties (URS and URB), the notional traded by the dealers with such counterparties and the notional arising from "hot potato" trades. The exposures deriving from these trades are computed as that notional amount in excess with respect to the notional needed to accommodate for the intermediation between URS and URS. The results are reported in figure 6: we observe that the largest amount of notional indeed originates from these trades. In particular, the amount of these trades is roughly 10 times the total amount traded with end-users, in line with the finding that very few dealers (≈ 12) dominate the central part of the bow-tie. The fifth and last result relates to the *robustness* of the SCC with respect to elimination of specific nodes. We compute a measure of *relative book mismatch* as the ratio between all the receivables on a reference entity (conditional to no counterparty default) and the gross exposure (Equation 14). We observe that the dealers' in the SCC, even the largest ones (which have positive out- and in-degree, i.e. the buy and sell risk at the same time), typically do not have completely matched books on each reference entity, unlike a CCP. In fact, these large dealer may be hedging in different ways, including the purchase of the underlying bond or by shifting risk across correlated reference entities. If a dealers offsets to zero its negative (positive) relative book mismatch by selling (buying) protection on the reference entity, then it no longer belongs to the SCC. We test the robustness of the SCC to these changes by progressively removing nodes with increasingly more matched books, as explained in detail in Appendix A.4. Even for very low levels of relative mismatch, we do not observe a disruption of the SCC for the vast majority of reference entities in time. We interpret this result as the confirmation of the existence of a small number of highly connected intermediaries (indeed the largest in terms of absolute notional traded) that create a very densely and strongly connected core within the SCC (Duffie et al., 2015).

3.3 Identification of the Ultimate Risk Sellers and Ultimate Risk Buyers

We now proceed with the analysis of the sets of URSs and URBs, i.e. the ultimate holder of counterparty and underlying credit risk respectively. We will start with a general "bird's eye" on the aggregate network and, then, "zoom-in" into the analysis of specific reference entities.

3.3.1 The aggregate network

In Figure 5, we can identify hedge funds to be the largest URS, immediately followed by asset managers. On the side of the URB, the situation changes, in that banks are the largest buyers of risk. The aggregate network does show large structural changes in time. A closer look to the classification of URS and URB is provided in Figure 7: we can see that hedge funds are the largest type of URSs and banks are the largest type of URBs in both snapshots. An important comment is in place for the aggregate network. The amount of risk sold by the URB does is much lower than the amount the amount sold by the URS because an URS on one entity who then buys protection on another, naturally becomes included in the
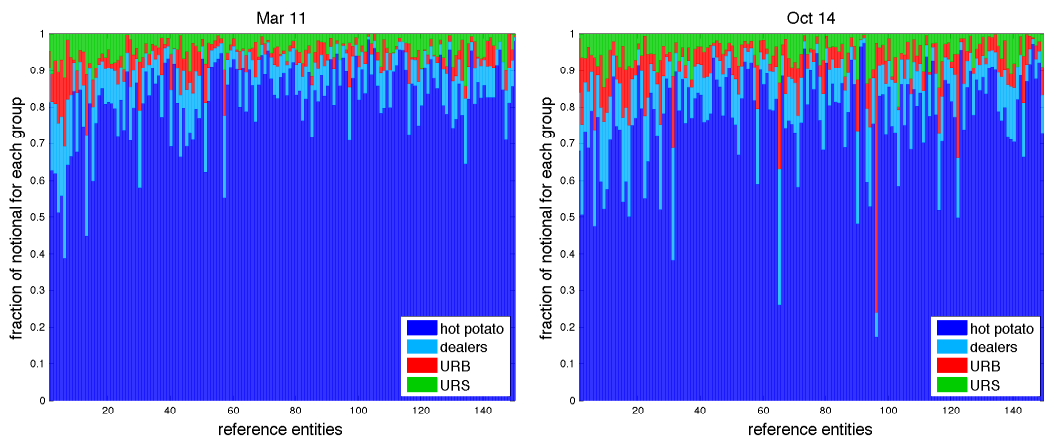
Figure 6: Decomposition of total notional traded. The graph shows the fraction of the total notional traded by URS (green), URB (red), dealer to either URS or URS (light blue) and the hot potato trades (dark blue) over the total notional traded for each reference entity. We have ordered the reference entities in descending order by total notional traded in each snapshot. We focus on the first 150 reference entities by total notional in both snapshot as some minor reference entities do not feature a bow-tie structure.

set of dealers. This implies that URS tend to have the same directionality on several reference entities, whereas not so many URBs keep this position on several reference entities.

An interesting result is the sharp increase in notional on the URB side for asset managers from the first to the fourth snapshot. From this graph, we can conclude that hedge funds have not modified their strategy. However, since we do not have data on the individual portfolio composition, e.g. bond holdings, we cannot draw definitive conclusions, which will be tackled in future work.

3.3.2 Zooming-in: URSs and URBs by reference entity category

When we *zoom-in* to specific reference entities, we can observe specific patterns in the way risk flows in the CDS market. In Figure 8, we visualise the network and the underlying flow-of-risk for a major sovereign and a major dealer for the snapshots March 2011 and October 2014. Despite the presence of a bow-tie structure in both snapshots for both reference entities, we can observe important differences in the way risk flows in time and along different reference entities. At first, we compare the flows for the major sovereign. We observe that hedge funds are the major URS in the first snapshot, whereas they become less important in the last snapshot. The structure of the URB does not vary much, except for the emergence of a large asset manager, holding the largest part of underlying credit risk. Therefore, we can say that, in March 11, a large part of fundamental risk flowed (via the dealers) from hedge funds to asset managers, whereas in Oct 14, the largest part of underlying credit risk flow originates from asset managers themselves and banks. This change in the composition of URS may be due to several reasons. These include, for instance, the EU regulation on short selling and uncovered (naked) CDS, which came into force in November 2012: EU institutions trading CDS on a sovereign entity must have a correspondent underlying exposure.[12]

Conversely, by comparing the flow for the reference entity "major dealer" in time, we do not find significant changes. The flow originates from asset managers (and, in particular a very large one) and ends with asset managers being the largest category of URBs. Also, we notice the presence of insurance companies, barely present for the major sovereign, on the side of URS. URS on the major dealer reference entity may to hedge their counterparty risk stemming from other positions, although we would need detailed data on their balance sheets in order to further confirm this claim.

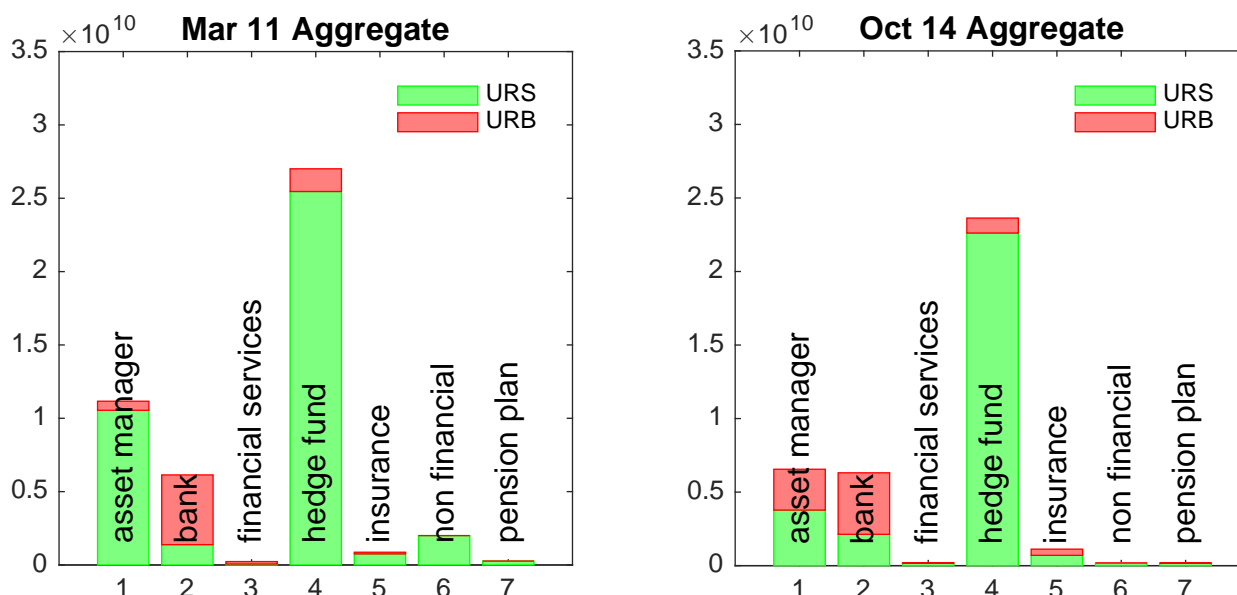[12]See https://www.esma.europa.eu/regulation/trading/short-selling and references therein for more details.

Figure 7: Notional traded by URS and URB divided by type. The total notional traded by the URS is in green and the total notional traded by the URB is in red.

Last, by comparing the flow in the two reference entities, we observe interesting results that show the potential of this type of analysis. By focusing on the March 11 snapshot, we observe that the main difference is that hedge funds rank as the first URS type, whereas the largest amount of protection on the major dealer was bought by asset managers. On the URB side, instead, we find asset managers to be the largest buyers of risk in both cases. These differences are made clear in Figure 9: despite the difference in the total notional (the major sovereign is roughly three times as big in terms of notional as the major dealer), it is clear the role of asset managers as risk buyers in the case of the major sovereign and as risk sellers in the case of the major dealer.

The discussion on the aggregate network and on the network based on two different reference entities shows that a certain degree of *heterogeneity* in the way risk flows can be found at the more granular level. We now analyse an intermediate level of aggregation, by considering the aggregate network of "all sovereigns" (typically the most traded reference entities) as the network capturing the "fundamental" credit risk as opposed to the aggregate network of "G-SIBS", capturing the flow of counterparty risk (e.g., when CDS are used as a hedging strategy).

By comparing the aggregate network "All sovereigns" in time, we do not observe significant differences, in terms of URS and URB, except for a general decline in the total notional. The comparison of the aggregate network "G-SIBS" in time, instead, shows an interesting change: asset managers become more important URB and less important URS on those reference entities. In other words, asset managers seek less protection on the G-SIBS dealers in October 14 than they did in March 11. The relative situation for the hedge funds does not vary significantly.

Last, we analyse the allocation of ultimate risk by type of reference entity. Figure 10 reports a bar plot with a decomposition of ultimate risk by type of reference entity. In particular, we observe a shift in the composition of the notional traded. Taking into account the general decline of the notional levels, we observe a clear change in where the flow-of-risk originates and ends up. In fact, we observe a relative increase of risk bought on EU periphery sovereigns and in other developed markets sovereigns. Also, we observe a relative decline in protection bought (sold risk) on the EU core sovereigns.

Further, by zooming-in on two specific types of reference entities (all sovereign entities and the G-SIBs), we observe how ultimate risk is distributed across the different counterparty types. In Figure 11, we report a bar plot of the notional amount held by URS and URB in March 11 and October 14 for the aggregate
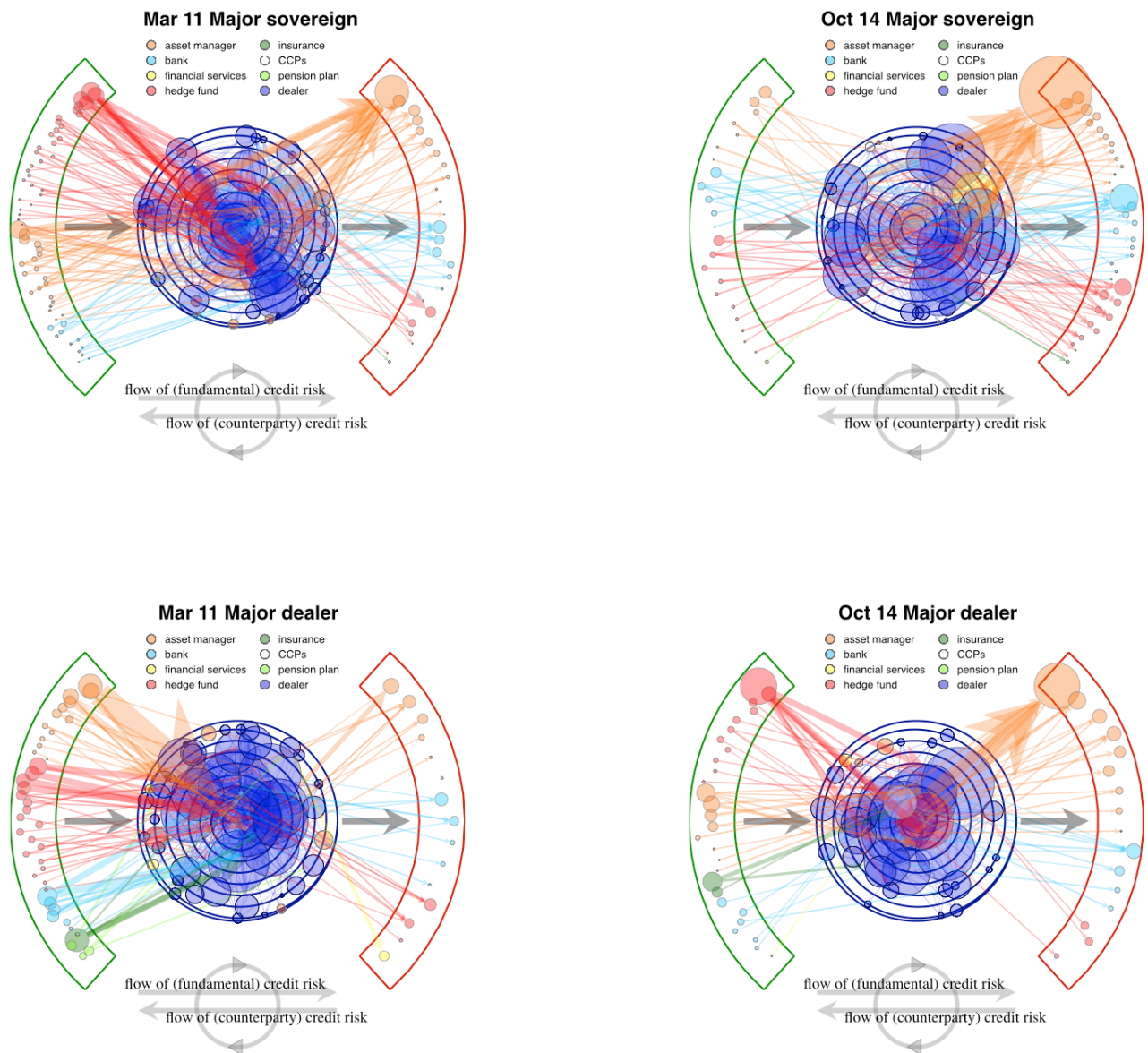
Figure 8: Upper figures: CDS network visualisations for a major sovereign, (Left) The network at March 11 and (right) the network at October 11. Lower figures: CDS network visualisations for a major dealer, (Left) the network at March 11 and (right) the network at October 11. The size of the nodes reflects the absolute gross notional traded (normalised by the the maximum within the respective component).

network composed by all sovereign entities and all G-SIBs entities. We observe that, both in March 11 and October 14, the largest ultimate protection buyers were hedge funds, and the largest protection sellers were asset managers, despite a general reduction of total notional traded. For the G-SIBs reference entity group, we observe a similar pattern of notional reduction. However, a marked difference is present: asset managers' positions as URB on G-SIBs almost quadruples between 2011 and 2014.

3.4 Ultimate Risk Buyers: portfolio and concentration analysis

In the previous parts of this Section, we focused on a detailed analysis at the level of specific (or aggregate) reference entities. In this part, we further narrow down our analysis and focus on the individual URBs and their portfolio composition. In particular, we study i) on which reference entities URBs are most
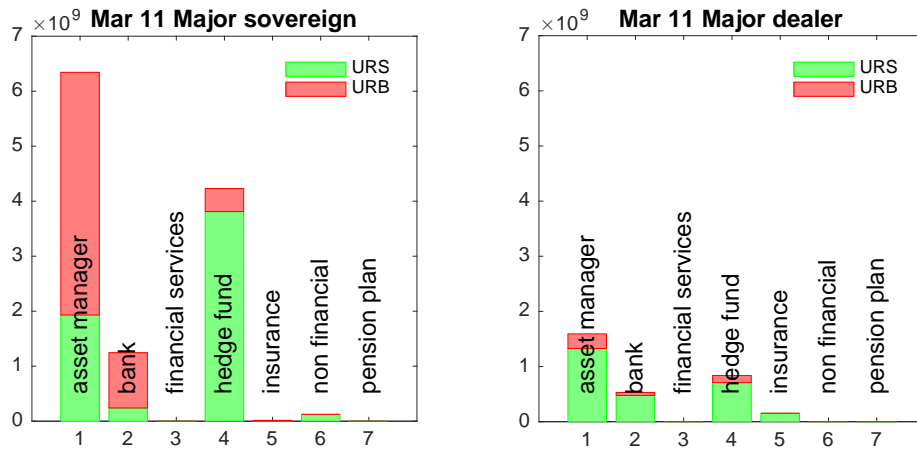
Figure 9: Bar plot of URS and URB on the major sovereign and major dealer for the March 11 snapshot.)
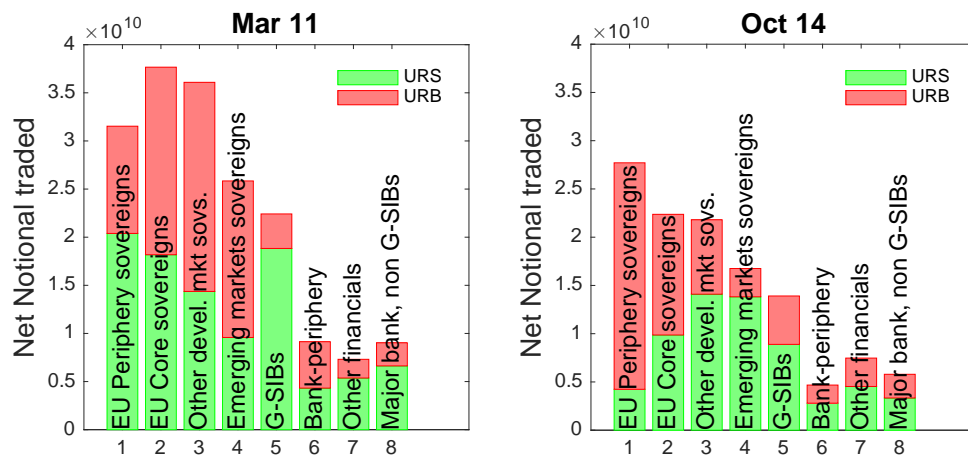

Figure 10: Bar plot of the allocation of ultimate risk (URS and URB) by type of reference entity for the two snapshots March 11 and October 14.
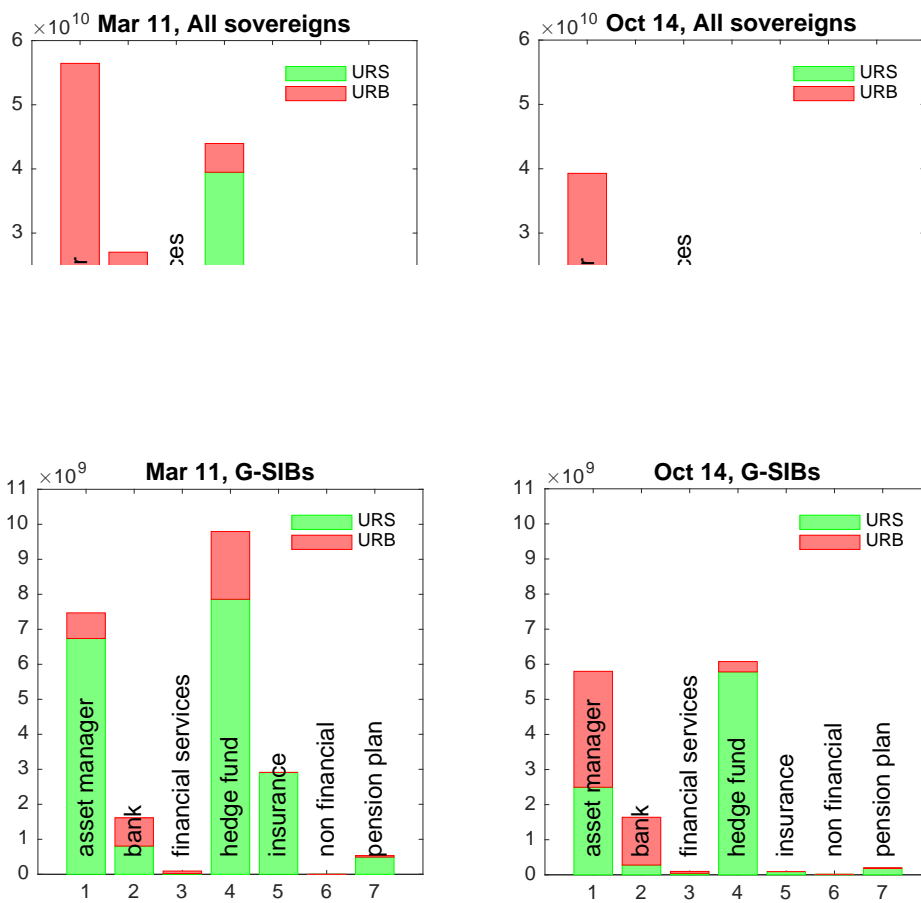
Figure 11: Bar plot of the notional traded by URS and URB for the aggregate network "All sovereigns" and the aggregate network "G-SIBS" for the two snapshots March 11 and October 14.

Table 4: Portfolio analysis of the largest URBs in March 11 and October 14. We rank the "first", "second" and "third" largest exposures as net buyers of risk in the CDS and report them by reference entity category.

March 11	1st	2nd	3rd
asset manager	Emerging markets sovs	EU Core sovs	Other devel. mkt sovs.
bank	EU Core sovs	EU Periphery sovs	EU Core sovs
hedge fund	EU Periphery sovs	EU Periphery sovs	EU Periphery sovs
bank	EU Periphery sovs	EU Core sovs	EU Core sovs
asset manager	EU Core sovs	EU Periphery sovs	EU Periphery sovs
bank	EU Periphery sovs	Emerging markets sovs	Other devel. mkt sovs.
bank	Other financials	EU Core sovs	Other devel. mkt sovs.
bank	Bank-periphery	EU Core sovs	EU Periphery sovs
bank	G-SIBs	G-SIBs	G-SIBs
bank	EU Periphery sovs	EU Periphery sovs	EU Periphery sovs

October 11	1st	2nd	3rd
asset manager	EU Periphery sovs	Emerging markets sovs	Emerging markets sovs
bank	EU Core sovs	EU Periphery sovs	EU Periphery sovs
hedge fund	Other financials	Other financials	Other financials
asset manager	EU Core sovs	EU Periphery sovs	G-SIBs
asset manager	EU Periphery sovs	Other financials	EU Periphery sovs
asset manager	Other devel. mkt sovs.	EU Core sovs	Other devel. mkt sovs.
asset manager	Other financials	Other financials	Other financials
hedge fund	EU Core sovs	EU Core sovs	EU Core sovs
bank	EU Core sovs	EU Core sovs	Other financials
bank	G-SIBs	G-SIBs	G-SIBs

exposed to and, ii) whether we observe a high level of concentration in the positions of URBs.

3.4.1 Portfolio analysis

We start by considering the ten largest URBs in March 11 and October 14. Table 4 reports the three largest exposures for each of these URBs. We show the results by group of reference entity. We observe that several leading URBs have indeed their largest exposures on sovereigns. We also find a bank that has its largest exposures on three different dealers.

However, the main result of this analysis is that the largest URBs typically have high *overlapped* position on similar reference entities. In other words, they have their largest exposures on potentially correlated reference entities, e.g. when two out of three of their largest exposures are on EU periphery sovereigns. Also, we find a bank specialised in offering protection on dealers, plus an asset manager and a hedge fund in October 14 heavily exposed to financials reference entities. This has particular implications in terms of systemic risk, as the co-movements of correlated reference entities, regardless of their default, can results in higher distress and margin calls, as in the AIG case. We will tackle this issue in more details in future work.

3.4.2 Concentration

The second main result stemming from the portfolio analysis it that URBs show a high degree of concentration of their portfolios. In other words, they are highly exposed to a limited number of reference entities.

Table 5: **Flow-of-risk concentration**. First column: number of leading URBs on the CDS network aggregated by subgroups. Second column: fraction of leading URBs for each reference entity subgroup with respect to the number of URBs for the subgroup. Third column: fraction of notional traded by the leading URBs in each subgroup. The networks for each subgroups are aggregated along the reference entities belonging to the subgroup as in Equation 3

March 11	# leading URBs	fraction of lead URBs	fraction of notional
EU Periphery sovereigns	4	0.14	0.82
EU Core sovereigns	2	0.07	0.87
Other developed mkts sovs	1	0.04	0.94
Emerging markets sovereigns	1	0.04	0.97
G-SIBS	9	0.26	0.57
Bank-periphery	3	0.09	0.78
Other financials	10	0.23	0.44
Major Bank-non dealer	7	0.32	0.65

October 14	# leading URBs	fraction of lead URBs	fraction of notional
EU Periphery sovereigns	1	0.02	0.89
EU Core sovereigns	3	0.09	0.74
Other developed mkts sovs	4	0.15	0.78
Emerging markets sovereigns	7	0.24	0.64
G-SIBS	16	0.29	0.41
Bank-periphery	4	0.13	0.71
Other financials	9	0.23	0.52
Major Bank-non dealer	12	0.3	0.47

In particular, we find that ultimate credit risk ends up in the hands of a few leading counterparties. To give a quantitative assessment of the level of concentration of ultimate credit risk, we focus - for the aggregated network by group G (Equation 3) of reference entity - on the top (leading) URBs. The number of *leading URBs* is computed as the nearest integer of the reciprocal of the Herfindahl index:

$$\#\text{leading URBs on group } G = \text{nint}\left(H_G^{-1}\right), \text{ where } H_G = \sum_i \left(\frac{a_{ij}^G}{\sum_{ij} a_{ij}^G}\right)^2. \tag{9}$$

Results are reported in Table 5 for two time snapshots (March 11 and October 14). The second column of the table shows the number of leading URBs in the network. The second and third column report, respectively, the fraction of leading URBs with respect to the total number of URBs on that reference entity group and the fraction of notional traded by those leading URB. The second and third column, in other words, reflect the Lorenz curve[13] for the total notional traded by the largest URBs. For example, on the EU periphery sovereign row for March 11, we observe a fraction of 14% leading URBs trading 82% of the total notional. With this analysis, we find that all reference entities groups are highly concentrated. The "G-SIBS" group shows a lower degree of concentration, where the ultimate risk appears to be spread between a higher number of URBs. A striking low number of URBs is present for the group "EU

---

[13]The Lorenz curve (Lorenz, 1905) is typically used to visualise and compute (Arcagni and Porro, 2014; D'Errico et al., 2015) the levels of concentration of wealth or income, by showing the proportion of the total variable associated to the a fixed bottom proportion of individuals. In our analysis, we consider its complement, i.e. we compute the proportion of overall notional held the top URBs

Table 6: **Statistics: flow-of-risk concentration**. The table shows the average number of URSs and URBs by group of reference entity. We also show the leading number of URSs and URBs according to the reciprocal of the Herfindahl index (Equation 9).

Mar 11	avg num URS	avg lead. URS	avg num URB	avg lead. URB
EU Periphery sovereigns	40.67	11.33	20.00	5.33
EU Core sovereigns	31.33	7.17	18.00	4.50
Other developed markets sovereigns	18.08	6.62	9.77	2.69
Emerging markets sovereigns	37.57	11.43	14.29	3.00
Dealers	31.07	8.27	19.60	9.07
Bank-periphery	17.58	6.58	12.83	5.58
Other financials	10.57	5.08	7.29	3.07
Major Bank-non dealer	12.45	5.55	8.80	4.80

Apr 12	avg num URS	avg lead. URS	avg num URB	avg lead. URB
EU Periphery sovereigns	34.17	7.67	20.00	5.83
EU Core sovereigns	44.17	13.17	23.83	5.83
Other developed markets sovereigns	20.08	7.23	9.15	2.38
Emerging markets sovereigns	38.00	10.00	15.00	2.57
Dealers	29.27	8.53	23.87	7.60
Bank-periphery	16.92	4.92	11.00	3.42
Other financials	10.61	5.07	7.45	2.61
Major Bank-non dealer	11.70	4.95	9.05	4.65

Dec 12	avg num URS	avg lead. URS	avg num URB	avg lead. URB
EU Periphery sovereigns	27.17	8.50	16.17	4.17
EU Core sovereigns	31.50	10.00	20.83	5.17
Other developed markets sovereigns	14.31	4.77	9.08	2.46
Emerging markets sovereigns	38.00	9.14	16.00	2.71
Dealers	27.13	7.00	24.53	9.00
Bank-periphery	15.83	4.33	9.50	3.75
Other financials	9.13	4.19	6.86	2.55
Major Bank-non dealer	10.55	4.35	8.80	4.65

Oct 14	avg num URS	avg lead. URS	avg num URB	avg lead. URB
EU Periphery sovereigns	16.83	6.50	16.33	3.00
EU Core sovereigns	19.33	6.83	16.33	4.00
Other developed markets sovereigns	11.46	3.92	7.38	2.23
Emerging markets sovereigns	36.29	9.86	16.43	1.57
Dealers	20.87	6.07	21.87	7.13
Bank-periphery	11.92	5.08	9.33	4.67
Other financials	6.48	2.93	5.99	2.58
Major Bank-non dealer	8.05	3.70	8.40	4.50

Periphery sovereigns". In particular, we observe only one leading URB on the EU periphery sovereign network, trading around 90% of the total URB notional. Overall, a common result is that the few leading URBs cover the striking majority of notional traded: we can therefore conclude that ultimate risk is

indeed heavily concentrated.

Last, we relate these results on concentration with the flow-of-risk statistics. Table 6 shows the statistics on the average leading URS and URBs for each reference entity considered individually. Results are reported again by reference entity group. Concentration occurs also on the URS side and help in understanding how much the flow-of-risk is concentrated from its origin in the URS towards their end in the URB. For example, for March 11, we observe on average 11 leading URS (origin of the flow) for the category "EU periphery" and the risk flow in the hands of (on average) 5 leading URB. In other words, we can conclude that the large amount of risk flows from 11 URS to 5 URB in that reference entity category. If we compare this result with the October 14 snapshot, we observe a further concentration of risk: the largest part of the notional starts from 6 URS and ends to 3 URB.

In summary, our main findings on the portfolio composition of the URBs can be outlined as follows. First, the largest part of risk traded originates in few URS and ends up in even less URBs. Second, we find that URBs show a high degree of portfolio concentration, in other words, they do not have diversified positions on the groups of reference entities. Third, asset managers constitute a large bulk of the risk held by URBs in terms of notional. Fourth, there are some URBs that are significantly exposed to potentially correlated groups of reference entities.

4 Concluding remarks

This paper provides a theoretical and empirical analysis of the structure of the network arising from the sequence of risk transfers in the CDS market. By introducing the notion of *flow-of-risk*, we develop a framework to analyse how both underlying credit and counterparty risks flow through the set of counterparties (Ultimate Risk Sellers - URS, Dealers, and Ultimate Risk Buyers - URB) in the network. We provide sufficient conditions for a bow-tie network architecture to emerge endogenously as the result of large intermediation levels (intra-Dealer trades) in the market. Furthermore, we show that a bow-tie network structure is particularly conducive to system-wide distress. In this network architecture, with strongly connected Dealers, the probability of a large loss due to materialisation of counterparty risk is higher than in more fragmented network structures.

From the empirical point of view, we find that a bow-tie network architecture is present for the majority of CDS reference entities over the four time snapshots. By detecting a bow-tie structure, we can univocally identify the counterparties at the beginning and the end of the flow-of-risk. For the aggregate CDS network, we find that hedge funds are generally the largest URSs, while asset managers and banks are the largest URBs. However, the results show more heterogeneity when it comes to a more disaggregated analysis at the reference entity level. Moreover, we find that the strongly connected component (SCC) of Dealers intermediates most of the notional (roughly 70%). This is an important finding, in terms of network analysis, since the fact that these counterparties are strongly connected implies that a potential counterparty distress originating in one node of the SCC or in the set of URBs can reach a very large fraction of other nodes in the network.

Furthermore, we find that the number of URBs is systematically lower than the number of URSs. In other words, underlying credit risk flows from a high number of risk sellers to a few risk buyers. We further analyse the level of concentration of ultimate risk, and find that very limited number of leading URBs for each reference entity. This high level of concentration suggests that, should the same URBs be heavily exposed to correlated risk via reference entities, this could engender higher levels of distress in case of a major credit event. Additionally, we find that non-banking institutions, such as asset managers, concentrate a large fraction of ultimate risk for particular classes of reference entities (including, e.g. large sovereigns), thereby pointing to the need to better understand their systemic relevance.

Our future research will aim at understanding different aspects related to the flow-of-risk. For example, given the large decline in notional traded, we wonder i) in which part of the flow-of-risk this reduction is taking place and whether this may be due to risk-mitigation technique such as compression or central clearing, and ii) whether this is affecting individual net positions, thereby understanding the motives

for engaging in these markets (Oehmke and Zawadowski, 2015a; Fontana and Scheicher, 2016). Another avenue of work, which we cannot fully carry out with our current anonymised sample, is related to measuring the extent to which risk flows are overlapped in the network. Overlap may, in fact, occur on two different levels: first, the same counterparties may be exposed to correlated reference entities; second, two reference entities may present similar sets of URS, dealers and URBs. Quantifying whether overlap is significant would help regulators in identifying institutions more vulnerable to common shocks on correlated reference entities. In this light, understanding how fundamental risk on G-SIBs (which could be aimed at hedging counterparty risk) overlaps with the underlying credit risk on different reference entities could help understand how institutions manage counterparty risk.

Moreover, our methodology to identify the flow-of-risk naturally lends itself to the analysis of other OTC derivative markets. For example, Interest Rate Swaps (IRS) and FX derivatives would be of significant interest. More generally, our analysis can be applied to any type of OTC network, including liquidity flows in interbank lending and payment systems.

From a broader perspective, the paper provides an example of how data from trade repositories can enhance the understanding, both from a research and policy perspective, of a complex OTC derivatives market such as the one for Credit Default Swaps. The availability of this type of data to regulators and policymakers is indeed one of the pillars[14] of the regulatory reforms the G20 leaders committed to in September 2009, in the aftermath of the global financial crisis. In the European Union, for instance, this is implemented via the European Markets Infrastructure Regulation (EMIR, 2012), and the research and policy work that has begun (see Abad et al., 2016, for an EU level analysis of EMIR data) aims at enhancing the transparency and the understanding of these markets.

---

[14]Alongside increased clearing for certain types of OTC derivatives via central clearing counterparties (CCPs).

References

Abad, J., Aldasoro, I., Aymanns, C., DErrico, M., Fache Rousová, L., Hoffmann, P., Langfield, S., Neychev, M., and Roukny, T. (2016). Shedding light on dark markets: first insights from the new EU-wide OTC derivatives dataset. *European Systemic Risk Board Occasional Paper*, no. 11.

Acemoglu, D., Ozdaglar, A., and Tahbaz-Salehi, A. (2015). Systemic Risk and Stability in Financial Networks. *American Economic Review*, 105(2):564–608.

Adrian, T., Shin, H. S., et al. (2008). Liquidity and financial contagion. *Banque de France Financial Stability Review: Special Issue on Liquidity*, 11:1–7.

Allahrakha, M., Glasserman, P., Young, H. P., et al. (2015). Systemic Importance Indicators for 33 U.S. bank holding companies: An Overview of Recent Data. *Office of Financial Research Brief Series*.

Allen, F. and Santomero, A. M. (1997). The theory of financial intermediation. *Journal of Banking & Finance*, 21(11):1461–1485.

Amihud, Y. and Mendelson, H. (1980). Dealership market: Market-making with inventory. *Journal of Financial Economics*, 8(1):31–53.

Arcagni, A. and Porro, F. (2014). The graphical representation of inequality. *Revista Colombiana de estadistica*, 37(2):419–437.

Arora, N., Gandhi, P., and Longstaff, F. A. (2012). Counterparty credit risk and the credit default swap market. *Journal of Financial Economics*, 103(2):280–293.

Barucca, P., Bardoscia, M., Caccioli, F., D'Errico, M., Visentin, G., Battiston, S., and Caldarelli, G. (2016). Network valuation in financial systems. *Available at SSRN 2795583*.

Basel Committee on Banking Supervision (2010). Basel III: A global regulatory framework for more resilient banks and banking systems. *Bank for International Settlements, Basel*.

Basel Committee on Banking Supervision (2015). Review of the Credit Valuation Adjustment Risk Framework. Consultative document, BCBS.

Battiston, S., Caldarelli, G., D'Errico, M., and Gurciullo, S. (2016a). Leveraging the network: a stress-test framework based on DebtRank. *Statistics & Risk Modeling*, 33(3-4):117–138.

Battiston, S., D'Errico, M., and Gurciullo, S. (2016b). DebtRank and the Network of Leverage. *The Journal of Alternative Investments*, 18(4):68–81.

Battiston, S., Puliga, M., Kaushik, R., Tasca, P., and Caldarelli, G. (2012). DebtRank: Too central to fail? Financial networks, the FED and systemic risk. *Scientific reports*, 2.

Benos, E., Wetherilt, A., and Zikes, F. (2013). The structure and dynamics of the UK credit default swap market. *Bank of England Financial Stability Paper*, 25.

Brigo, D. and Chourdakis, K. (2009). Counterparty risk for credit default swaps: Impact of spread volatility and default correlation. *International Journal of Theoretical and Applied Finance*, 12(07):1007–1026.

Broder, A., Kumar, R., Maghoul, F., Raghavan, P., Rajagopalan, S., Stata, R., Tomkins, A., and Wiener, J. (2000). Graph structure in the web. *Computer networks*, 33(1):309–320.

Brunnermeier, M., Laurent, C., El Omari, Y., Gabrieli, S., Kern, S., Memmel, C., Peltonen, T., Podlich, N., Scheicher, M., and Vuillemey, G. (2013). Assessing contagion risks in the CDS market. *Banque de France, Financial Stability Review*, 17:123–134.

Brunnermeier, M. K. (2009). Deciphering the liquidity and credit crunch 2007–2008. *The Journal of Economic Perspectives*, 23(1):77–100.

Burnham, J. (1991). Current structure and recent developments in foreign exchange markets. *editor: S. Khoury, Recent Developments in International Banking and Finance*, pages 123–153.

Campbell, S. and Gallin, J. (2014). Risk Transfer Across Economic Sectors Using Credit Default Swaps. *FEDS Notes*.

Castrén, O. and Kavonius, I. K. (2009). Balance sheet interlinkages and macro-financial risk analysis in

the euro area. *European Central Bank Working Paper series*.

Clerc, L., Gabrieli, S., Kern, S., and El Omari, Y. (2013). Assessing contagion risk through the network structure of CDS exposures on European reference entities. In *AFSE Meeting 2013*.

Cont, R. (2010). Credit default swaps and financial stability. *Banque de France, Financial Stability Review*, 14.

Cont, R. and Minca, A. (2015). Credit default swaps and systemic risk. *Annals of Operations Research*, pages 1–25.

Craig, B. and Von Peter, G. (2014). Interbank tiering and money center banks. *Journal of Financial Intermediation*, 23(3):322–347.

Crosbie, P. and Bohn, J. (2003). Modeling default risk. *KMV working paper*.

D'Errico, M., Macchiarelli, C., and Serafini, R. (2015). Differently unequal: Zooming-in on the distributional dimensions of the crisis in euro area countries. *Economic Modeling*, 48:93–115.

D'Errico, M. and Roukny, T. (2016). Compressing over-the-counter markets. Forthcoming.

Duffie, D., Gârleanu, N., and Pedersen, L. H. (2005). Over-the-Counter Markets. *Econometrica*, 73(6):1815–1847.

Duffie, D., Scheicher, M., and Vuillemey, G. (2015). Central clearing and collateral demand. *Journal of Financial Economics*.

Eisenberg, L. and Noe, T. H. (2001). Systemic risk in financial systems. *Management Science*, 47(2):236–249.

Elliott, M., Golub, B., and Jackson, M. O. (2014). Financial Networks and Contagion. *American Economic Review*, 104(10):3115–3153.

Erdős, P. and Rényi, A. (1959). On random graphs I. *Publ. Math. Debrecen*, 6:290–297.

European Central Bank (2009). Credit Default Swaps and Counterparty Risk. `https://www.ecb.europa.eu/pub/pdf/other/creditdefaultswapsandcounterpartyrisk2009en.pdf`.

Even, S. (2011). *Graph algorithms*. Cambridge University Press.

Fender, I., Frankel, A., and Gyntelberg, J. (2008). Three market implications of the Lehman bankruptcy. *BIS Quarterly Review*, pages 6–7.

Flood, M. D. (1994). Market structure and inefficiency in the foreign exchange market. *Journal of International Money and Finance*, 13(2):131–158.

Fontana, A. and Scheicher, M. (2016). An analysis of euro area sovereign cds and their relation with government bonds. *Journal of Banking & Finance*, 62:126–140.

Fricke, D. and Roukny, T. (2016). Generalists and specialists in the credit market. *Available at SSRN 2752413*.

Friedkin, N. E. (1991). Theoretical foundations for centrality measures. *American Journal of Sociology*, pages 1478–1504.

Giglio, S. (2012). Credit default swap spreads and systemic financial risk. *Booth Research Paper No. 12-45; Fama-Miller Working Paper, Available at SSRN 2023108*.

Glasserman, P. and Young, H. P. (2015). How likely is contagion in financial networks? *Journal of Banking & Finance*, 50:383–399.

Haldane, A. G. (2009). Rethinking the financial network. Speech delivered at the Financial Student Association, Amsterdam, The Netherlands.

Hansch, O., Naik, N. Y., and Viswanathan, S. (1999). Preferencing, internalization, best execution, and dealer profits. *The Journal of finance*, 54(5):1799–1828.

Harary, F. (1969). *Graph theory*. Westview Press.

Hollifield, B., Neklyudov, A., and Spatt, C. S. (2014). Bid-Ask Spreads, Trading Networks and the Pricing of Securitizations: 144a vs. Registered Securitizations. *Trading Networks and the Pricing of*

Securitizations: 144a vs. Registered Securitizations (August 2014).

Hull, J. C. (2014). *Options, futures, and other derivatives.* Pearson, ninth edition.

Hull, J. C. and White, A. (2000). Valuing credit default swaps I: no counterparty default risk. *Journal of Derivatives*, 8:29–40.

Hull, J. C. and White, A. (2001). Valuing credit default swaps II: modeling default correlations. *Journal of Derivatives*, 8:12–22.

ISDA (2014). Credit Derivatives Definitions.

Jarque, C. M. and Bera, A. K. (1987). A test for normality of observations and regression residuals. *International Statistical Review/Revue Internationale de Statistique*, pages 163–172.

Katz, L. (1953). A new status index derived from sociometric analysis. *Psychometrika*, 18(1):39–43.

Knuth, D. E. (1998). *The art of computer programming: sorting and searching*, volume 3. Pearson Education.

Krackhardt, D. and Hanson, J. R. (1993). Informal networks. *Harvard Business Review*, 71(4):104–111.

Li, D. and Schürhoff, N. (2014). Dealer networks. *CEPR Discussion Paper No. DP10237.*

Lorenz, M. O. (1905). Methods of measuring the concentration of wealth. *Publications of the American statistical association*, 9(70):209–219.

Lyons, R. K. (1995). Tests of microstructural hypotheses in the foreign exchange market. *Journal of Financial Economics*, 39(2):321–351.

Lyons, R. K. (1997). A simultaneous trade model of the foreign exchange hot potato. *Journal of International Economics*, 42(3-4):275–298.

Mengle, D. (2010). The importance of close-out netting. *ISDA Research Notes*, 1.

Merton, R. C. (1974). On the pricing of corporate debt: The risk structure of interest rates. *The Journal of Finance*, 29(2):449–470.

Oehmke, M. and Zawadowski, A. (2015a). Synthetic or real? the equilibrium effects of credit default swaps on bond markets. *Review of Financial Studies*, page hhv047.

Oehmke, M. and Zawadowski, A. (2015b). The anatomy of the CDS market. *Review of Financial Studies (forthcoming).*

Peltonen, T. A., Scheicher, M., and Vuillemey, G. (2014). The network structure of the CDS market and its determinants. *Journal of Financial Stability*, 13:118–133.

Plantin, G., Sapra, H., and Shin, H. S. (2008). Marking-to-Market: Panacea or Pandora's Box? *Journal of accounting research*, 46(2):435–460.

Reiss, P. and Werner, I. (1998). Does risk sharing motivate interdealer trading? *Journal of Finance*, LIII(5):1657.

Shachar, O. (2012). Exposing the exposed: Intermediation capacity in the credit default swap market. *Working Paper, NYU Stern.*

Stiglitz, J. E. (2010). Risk and global economic architecture: Why full financial integration may be undesirable. *American Economic Review*, 100(2):388–92.

Stulz, R. M. (2010). Credit default swaps and the credit crisis. *Journal of Economic Perspectives*, 24(1):73–92.

Visentin, G., Battiston, S., and D'Errico, M. (2016). Rethinking Financial Contagion. *Available at SSRN 2831143.*

Vitali, S., Glattfelder, J. B., and Battiston, S. (2011). The network of global corporate control. *PLoS-ONE*, 6.

Zawadowski, A. (2013). Entangled financial systems. *Review of Financial Studies*, 26(1):1291–1323.

Zhong, Z. (2014). The Risk Sharing Benefit versus the Collateral Cost: The Formation of the Inter-Dealer Network in Over-the-Counter Trading. *Available at SSRN 2318925.*

A Appendix

A.1 Graph theory: notation, definitions, and preliminary results

We will hereby provide some useful definitions and results of graph theory.[15] A *graph* $G = (V, E)$ is a collection of two sets: V is the set of nodes and E is the set of edges. Unless otherwise stated, n is number of nodes, and m is the number of edges. The CDS graph is *directed*, i.e. all edges are *ordered* pairs (i, j) of nodes (counterparties). In our setting, an ordered edge (i, j) represents the transfer of fundamental (credit) risk from i to j (along a specific reference entity). In our construction of the CDS network, exposures are bilaterally netted and therefore the existence of a link (i, j) implies that (j, i) does not exist. The *transpose* of a graph $G = (V, E)$ is a graph $G' = (V, E')$ where the set of edges E' is obtained by reversing the orientation of the edges in E: $E' = \{(i, j) : (j, i) \in E\}$.

The *in-degree* deg_i^{in} of a node i is the number of links pointing to i, whereas the *out-degree* deg_i^{out} is the number of links pointing to other nodes from i. The *density* of a graph is the ratio between the number of edges and the total possible number of edges $\delta = \frac{|L|}{n(n-1)}$.

Reachability   A *path* from i to j, denoted by $i \to j$, is an ordered sequence of edges and nodes in the graph with initial node i and ending node j. By transitivity, if $i \to j$ and $j \to l$ then $i \to l$. A *cycle* is a path of any length from i to itself ($i \to i$). Notice that $i \to j$ does not necessarily imply $j \to i$. The *length* of the path is the number of edges in a path. The *shortest path* (also called *geodesic*) between any two nodes i and j is the path (if any) with the minimal length. The length of the shortest path between i and j is said to be the *distance* of i from j. If there exists no path between i and j, then the distance is infinite. The *diameter* of a graph is defined as the largest distance between any two nodes. The *reachability set* R_i of a node i is the set of those nodes j for which there exist a path $i \to j$; formally:

$$R_i = \{j \in V : i \to j\}.$$

A straightforward but important consequence of the definition of reachability set is that $j \in R_i \implies R_j \subseteq R_i$ and, therefore:

$$R_i = \bigcup_{j \in R_i} R_j$$

Also, let N_i be the set of direct neighbours of i (i.e. the nodes in the reachability set of i with unitary distance, i's direct counterparties in the CDS market) of each node $i \in V$. By exploiting the definition of reachability, one can determine the reachability set of any i by means of the following recursive expression:

$$R_i = \left\{ N_i \cup \bigcup_{j \in N_i} R_j \right\}. \tag{10}$$

Equation 10 shows how the i's reachability set can be decomposed into the set of i's direct counterparties (i.e., from a risk management perspective, the counterparties of which i monitors the riskiness) and i's indirect counterparties.

Connectivity   The concept of *connectivity* is fundamental in our approach. A *strongly connected component* (SCC) is a set of nodes $V^{\mathrm{scc}} \subseteq V$ such that $\forall \{i, j\} \in V^{\mathrm{scc}}, i \to j$. Notice that, for all pairs of nodes i, j in the SCC, it holds that $i \to j$ and $j \to i$; therefore the reachable sets of all nodes in the SCC coincide: $R_i \supseteq V^{\mathrm{scc}}, \forall i \in V^{\mathrm{scc}}$. A strongly connected (SC) graph is a graph composed of one and only one strongly connected component, i.e. $V^{\mathrm{scc}} = V$.

---

[15]The reader can find further details about graph theory in Harary (1969).

A.1.1 Useful lemmas

LEMMA 1 (Probability of obtaining a strongly connected graph). *The probability that a graph $G = (V, E)$ is strongly connected is non-decreasing w.r.t. to the number of links.*

Proof. By definition, G is strongly connected iff $\forall i, j \in V \Rightarrow i \in R_j$. First, suppose G is not strongly connected, then $\exists (i, j)$ s.t.$i \notin R_j$. The new reachability set $R_j^{(i,v)}$ obtained by adding an additional edge (i, v) is always such that $R_j^{(i,v)} \supseteq R_j$, and therefore can only increase R_j. Last, when G is strongly connected, adding a link to G does not reduce the reachability set of any node and therefore G remains strongly connected. ∎

LEMMA 2 (Emergence of a cycle). *Consider a graph $G = (V, E)$, with $n = |V| \geq 2$. If each node i has strictly positive out- and in- degree ($deg_i^{in} > 0$ and $deg_i^{out} > 0$), then $\forall i \in V$, there exists at least one cycle containing i.*

Proof. The proof consists of two steps.

1. Consider the case $deg_i^{\text{in}} = deg_i^{\text{out}} = 1$. Since i has one outgoing edge and one incoming edge, its outgoing edge coincides with another node's incoming edge. Considering the nodes in the reachability set of i, we always find at least one node j whose outgoing edge coincides with i's incoming edge. Therefore there is always at least one path $i \rightarrow i$, which means that i belongs to at least one cycle.

2. Since the probability of obtaining SCC is non-decreasing w.r.t. the addition of links, we can add an arbitrary number of links to the graph, and therefore any node can have arbitrary in-degree and out-degree.

∎

LEMMA 3 (Union of non-disjoint cycles). *The union of any number of non pairwise-disjoint cycles is strongly connected.*

Proof. We start by proving that the lemma holds in the case of two cycles having at least one node i in common. In this case, i is reachable from and can reach any other node in either cycles. Therefore, by transitivity, each node in either cycles is reachable from any node in either cycles. If a graph G contains more than two non pairwise-disjoint cycles, then there is a path from any node in any cycle to any other node and G is strongly connected. ∎

DEFINITION 1 (Bow-tie network architecture). *A graph $G(V, E)$ has a bow-tie architecture if and only if V can be partitioned into three disjoint sets of nodes IN, SCC, OUT such that:*

1. *SCC is strongly connected, and it is the only strongly connected subset in the graph;*

2. *all nodes in IN can reach SCC but cannot be reached from it, these nodes are the upstream nodes in the graph;*

3. *OUT nodes can be reached from SCC but cannot reach it. These nodes are "downstream" in the graph.*

In other words, identifying a bow-tie structure attempts at finding a permutation matrix Q such that the permutation of the original matrix A has the following blocks structure:

$$A^P = QAQ^\top = \begin{bmatrix} 0 & A_{\text{IN, SCC}} & 0 \\ 0 & A_{\text{SCC, SCC}} & A_{\text{SCC, OUT}} \\ 0 & 0 & 0 \end{bmatrix}. \tag{11}$$

where, since the SCC is strongly connected, the block $A_{\text{SCC, SCC}}$ is irreducible.

A.1.2 Bow-tie detection algorithm

The algorithm we use to detect a bow-tie architecture and identity its components is based on graph traversal algorithm such as Depth First Search (DFS) and Breadth First Search (BFS) (Knuth, 1998; Even, 2011). We hereby give a qualitative description of the algoritm:[16]

1. find the Strongly Connected Components of G via a DFS, if there exists more than one SCC, then the graph is not a bow-tie

2. run a BFS on all nodes $\in V^{\mathrm{SCC}}$ and find all nodes downstream (the OUT component)

3. run a BFS on all nodes $\in V^{\mathrm{SCC}}$ after reversing link directions and find all nodes upstream (the IN component).

A.2 Re-evaluation of counterparty risk

In this appendix, we formalise the distress propagation model in a CDS network. The main idea behind the model is that a loss originating in *any* counterparty in the CDS market spreads, in a mark-to-market framework, to its other direct counterparties. and can potentially spread further along the main direction of the flow-of-risk.

Mark-to-market value with counterparty risk First, we need to compute the value of a CDS contract in a mark-to-market framework. A CDS is a contingent claim in which *both* the underlying reference entity and the counterparty may default. Let a_{ijk}, as defined in Equation 1, be the notional amount of a contract. Also, denote with $p(k)$ and $p(j)$ the probability of default of k and j, respectively; $p(j,k) = p(k,j) = p(j|k)p(k)$ is the probability of joint default of j and k. When the underlying entity k defaults, the protection seller j pays the notional amount a_{ijk}, upon delivery of one of k's defaulted bonds (this is referred to as "physical settlement" of the CDS contract). It is important to recall that, in general, i does not need to posses the underlying bond. When there is limited availability of the defaulted entity's bonds in the market, an auction determines the k's bond's recovery rate and determines the amount that is cash-settled(see, e.g., Hull and White, 2000, 2001; Hull, 2014; ISDA, 2014). We denote the recovery rate after the auction by ρ_k. If k defaults and j does not, then i receives a payment from j on the remaining fraction $(1 - \rho_k)$. When both k and j default, then the payoff for i is determined also by the recovery rate of j, ρ_j (not necessarily due to an auction process). When k does not default, no payment from j is expected. This is summarised in the table below:

j	k	payoff	probability
default	default	$\rho_j (1 - \rho_k) a_{ijk}$	$p(j,k)$
non default	default	$(1 - \rho_k) a_{ijk}$	$p(k) - p(k,j)$
default	non default	0	$p(j) - p(j,k)$
non default	non default	0	$1 - [p(k) + p(j) - p(j,k)]$

The expected payoff for each counterparty i in the neighbour set N_j of j, i.e. the mark-to-market value, can be written as follows

$$\forall i \in N_j : \quad M_{ijk} = a_{ijk} \left(\rho_j(1 - \rho_k)p(j,k) + (1 - \rho_k)(p(k) - p(k,j)) \right)$$
$$= a_{ijk} \, p(k) \, (1 - \rho_k) \, (1 - (1 - \rho_j)p(j|k)) \tag{12}$$

---

[16]The algorithm's complexity is driven by the DFS's complexity, $O(|V| + |E|)$.

where we have written the payoff in terms of the conditional probability of default. [17] This allows to make explicit the positive dependence on $p(k)$ and the negative dependence on $p(j|k)$. The higher the probability of default of the counterparty conditional upon the default of the reference entity, the lower the expected payoff.

In the paradigmatic case when recovery rates are set to zero (for instance, in the very short run after the default event) and the default events are independent, we can write the market value as follows:

$$\forall i \in N_j : \quad M_{ijk}^{\text{ind}} = a_{ijk}p(k)(1 - p(j)) \quad \text{[independence of defaults of } j \text{ and } k\text{]}$$

which simplifies the formula and makes explicit how an increase in the default probability of j reduces the mark-to-market value of the contract.

A.3 Theoretical results on systemic distress

Proof of Theorem 1

Proof. We start by proving that $P_{\text{ind}}^{\text{syst}} \leq P_{\text{ind}}^{\text{syst}}$. For this to hold true, it suffices that, for each possible configuration of C_1, the reachable set R_i of any $i \in C_1$ in the case of independent chains is always contained in the reachable set of any $i \in C_1$ in the case of semi-independent chains. In the case of independent chains, the R_i comprise the dealers along the chains and the URS. In the case of interdependent chains, it comprises *at least* the same dealers and might include more dealers and URBs. Therefore:

$$P_{ind}^{syst} \leq P_{weak}^{syst} \leq P_{bowtie}^{syst}.$$

∎

Proof of Theorem 2

Proof. We need to show that there always exists a directed *path*, i.e. a series of distinct adjacent nodes in the CDS exposures network such that the starting nodes is the URS i and the last node is the URB j. Since:

1. there exist a path (i, d_1) of length one (one link) between each URS i and *at least* one dealer d_1

2. there exist a path (d_2, j) of length one (one link) between *at least* one dealer d_2 and the selected URS j:

3. there exists at least one directed path (with no specific length) $(d_1, \ldots, d_2)$ between each dealer d_1 and d_2

then there exists the path $(i, d_1, \ldots, d_2, j)$ from i to j.

∎

Proof of Theorem 3

Proof. Because of assumption A1, each i must lie in at least one cycle. In a very basic setting, we assume that presence of an edge between occurs with a certain probability, as in an ER (Erdős and Rényi, 1959) random graph model. We know that the undirected version of an ER graph as a connectivity threshold for its density $\delta > \frac{\log(n)}{n}$, as n increases. This implies that G is weakly connected if the number of links is larger than $\delta \times n(n-1) = \frac{\log(n)}{n} \times n(n-1) = (n-1)\log(n)$. If G is weakly connected, then there is a path (regardless of the direction) from any i to any j. This implies that all the cycles in the graph are surely non pairwise disjoint. Since every node lies in at least one cycle, it means that the graph is also strongly connected. ∎

---

[17]Notice that this pricing model for the protection leg of a CDS is a simplified version of more complex models (Hull and White, 2001; Brigo and Chourdakis, 2009), which take into account other important factors, such as default correlation and credit spread volatility. Giglio (2012) proposes an interesting method to measure the joint defaults of large financial institution in the market and provides bounds on the probabilites based on information inferred from credit default swaps.

REMARK 1 (Hot potato notional). *In case of dealers with matched books with URBs and URSs, there is always a configuration allowing for an arbitrarily high level of notional traded.*

Figure 12 show how, in the presence of matched books with end users, the inter-dealer trades can be arbitrarily large. This is due to presence of a strongly connected component connecting the dealers (in blue) in a cycle.
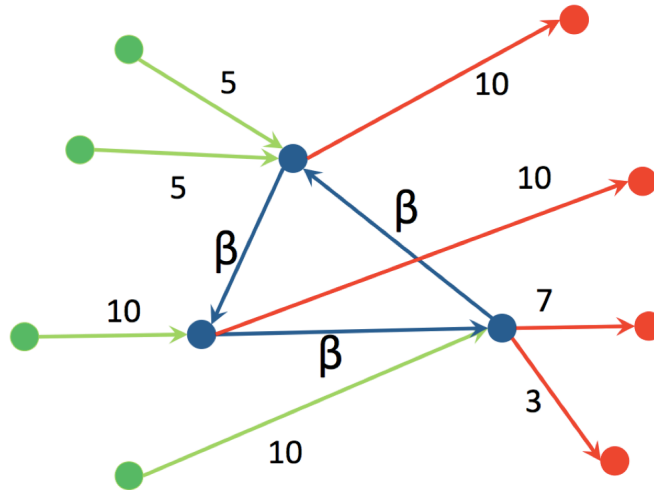

Figure 12: Size of "hot potato" trades. In the presence of matched books with end users (in green, the URS and, in red, the URBs), the dealers (in blue) can have arbitrarily large positions within themselves.

A.4 Robustness of the bow-tie network architecture

The block-model reported in Equation 11 represents a very specific block structure for the adjacency matrix and, consequently, for the correspondent network structure. This implies that, in general, a departure from that specific block form would not map into a bow-tie architecture for the associated network. Here, we analyse the robustness of the bow-tie model to our data by focusing on two aspects: i) we compute an error score due to the presence of non-zero element in the block structure in the blocks where those are not expected; ii) we test the robustness of the bow-tie structure versus a change in the topological roles of the nodes in the SCC.

Error score For each reference entity k and snapshot t, we adopt an approach similar to that of Craig and Von Peter (2014) and Fricke and Roukny (2016). We count the number of links we observe in the six zero-blocks of Equation 11, i.e. $A_{\text{IN, IN}}$ $A_{\text{SCC, IN}}$, $A_{\text{OUT, IN}}$, $A_{\text{OUT, SCC}}$, $A_{\text{OUT, OUT}}$. For each reference entity k at each time snapshot t, we then compute the total error score as follows:

$$\epsilon_{TOT}^{k,t} = e_{\text{IN, IN}}^{k,t} + e_{\text{SCC, IN}}^{k,t} + e_{\text{OUT, IN}}^{k,t} + e_{\text{OUT, SCC}}^{k,t} + e_{\text{IN, OUT}}^{k,t} + e_{\text{OUT, OUT}}^{k,t}$$

For all reference entities and time snapshots, we find no links in the blocks $A_{\text{SCC, IN}}$, $A_{\text{OUT, IN}}$, $A_{\text{OUT, SCC}}$. The total error score can then be decomposed in the following three remaining components:

$$\epsilon_{TOT}^{k,t} = \epsilon_{\text{IN, IN}}^{k,t} + \epsilon_{\text{IN, OUT}}^{k,t} + \epsilon_{\text{OUT, OUT}}^{k,t}$$

The results strongly confirm the presence of a bow-tie in the CDS network. Results are reported in Figure 13 We obtain a zero error score for a total of $129, 127, 115, 118$ over the 162 reference entities for the snapshots March 2011, April 12, December 12, and October 14 respectively. This implies that, for more than 70% (85% percent of the notional in our sample) of the reference entities a bow-tie is found with absolute precision. These reference entities are typically the largest in terms of traded notional and
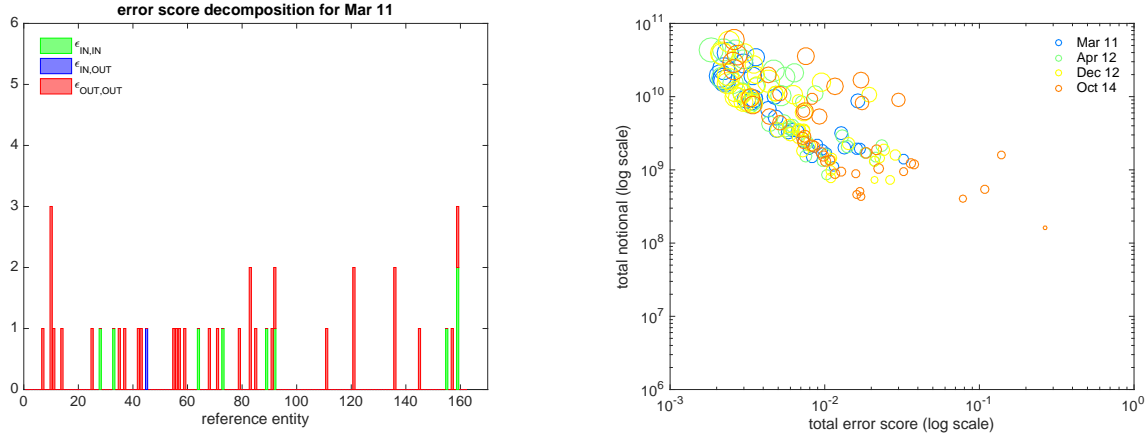
Figure 13: (Left) Error score decomposition, green, blue and red bars reflect the fraction of IN, IN links, IN, OUT links, OUT, OUT links as a fraction of total links. (Right) Normalised error score (log scale) vs notional of the reference entity (log scale).

include all the major global sovereigns and financials. Further, it is important to notice that the reference entities for which we observe a positive error score have typically experienced distress or credit events and the overall trading activity has dropped to very few outstanding trades. Further, the vast majority of non-zero error scores are due to trade between nodes in the out component (i.e. the URBs). Typically the number of links that do not fit a bow-tie are between 1 and 2. The figure on the right hand side compares the error score for different reference entities in time (both in log-scale). On the x-axis we computed the error score normalised by the number of links for each reference entity in the snapshot. The results show very low normalised error scores for largely traded reference entities.

Robustness of the SCC The random graph model we propose in this work is based on a density argument: the more "hot potato" trades, the more the number of links in the dealer subnetwork which leads, in turn, to a higher probability of obtaining a bow-tie. However, we wonder how *robust* such network architecture is with respect to a reduction in the number of trades within the strongly connected component of the bow-tie.

The key quantity for this analysis is the *relative book mismatch* b_{ik}, $\forall (i, k)$, computed as follows:

$$b_{ik} = \frac{\text{receivables on } k - \text{payables on } k}{\max \{\text{receivables on } k, \text{payables on } k\}} = \frac{\sum_j a_{ijk} - \sum_j a_{jik}}{\max \left\{ \sum_j a_{ijk}, \sum_j a_{jik} \right\}} \in [-1, 1]. \tag{13}$$

Equation 13 measures the relative net fundamental risk transferred by node i on reference entity k. The numerator can be interpreted as the amount of money i receives in case of default of k and no default of any of its counterparties. We further tested the normality of the net positions $\sum_j a_{ijk} - \sum_j a_{jik}$ for each reference entity k for each snapshot by performing a Jarque-Bera test (Jarque and Bera, 1987): we can reject the hypothesis of normality at the 5% significance level in about 90% of the reference entities

consistently in time. By construction, we have:

$$b_{ik} = \begin{cases} 1 & \text{for all URSs,} \\ \in (-1, 1) & \text{for all nodes in the SCC (dealers),} \\ -1 & \text{for all URBs.} \end{cases} \qquad (14)$$

We then implement, for each reference entity k and for each time-snapshot t, the following algorithm:

Initialisation: Set $\theta > 0$ arbitrarily small. Initialise the set of nodes $U = V_{\text{SCC}}$, U is the only strongly connected component.

Step 1: Compute b_{ik}, $\forall i \in U$.

Step 2: Remove from U all nodes such that $|b_{ik}| > 1 - \theta$. This moves the selected nodes either to the set of URS or URB.

Step 3: Perform the bow-tie analysis and compute the *number* of strongly connected components.

Step 4: Increase θ and repeat the procedure.

In our implementation, we set the initial threshold equal to 0.1 and we stop the iteration at 0.9. The idea behind this procedure is to incrementally "move out" of the SCC those nodes that are closer to being either in the IN our OUT component in order to "break" the strongly connected component.

For sake of brevity, we do not report the whole set of results of our robustness analysis. As an example of the analysis, consider Table 7, which reports the number of strongly connected components we find for different values of θ. In particular, we focus on the first 15 largest reference entities for the first snapshot (March 2011). The table lists the 15 most traded reference entities and the number of strongly connected components found for incremental values of θ. We find two main results for all the different snapshot. First, the threshold for which the bow-tie topology is disrupted lies within $0.3 - 0.5$ for the vast majority of reference entities. Second, the least traded reference entities are those for which we observe a disruption of the bow-tie structure for lower values of θ. Since we are only dealing with nodes in the SCC, these results reinforce our argument about how increasing "hot potato" trades as a sufficient condition for the emergence of a bow-tie structure.

Table 7: Robustness analysis for the SCC. The table reports the number of strongly connected components for the top 15 reference entities for different values of the threshold θ.

$\theta =$	0.1	0.2	0.3	0.4	0.5	0.6	0.7	0.8	0.9
Ref entity 1	1	1	2	2	3	4	4	5	5
Ref entity 2	1	1	2	2	2	2	4	5	5
Ref entity 3	1	1	1	1	1	1	1	1	3
Ref entity 4	1	1	1	2	3	3	7	7	8
Ref entity 5	1	1	1	2	3	5	6	6	6
Ref entity 6	1	1	1	1	1	1	6	6	8
Ref entity 7	1	1	1	3	4	4	4	6	6
Ref entity 8	1	1	1	1	1	3	6	6	11
Ref entity 9	1	1	2	1	1	1	4	8	12
Ref entity 10	1	1	1	1	2	2	2	3	7
Ref entity 11	1	1	1	2	3	5	5	6	9
Ref entity 12	1	1	1	1	3	3	10	10	10
Ref entity 13	1	1	1	1	1	1	1	1	7
Ref entity 14	1	1	1	2	3	8	9	9	13
Ref entity 15	1	2	2	2	2	2	3	6	7

Marco D'Errico
Department of Banking and Finance, University of Zurich, Zürich, Switzerland; email: marco.derrico@uzh.ch

Stefano Battiston
Department of Banking and Finance, University of Zurich, Zürich, Switzerland; email: stefano.battiston@uzh.ch

Tuomas Peltonen
European Systemic Risk Board, Frankfurt am Main, Germany; email: tuomas.peltonen@esrb.europa.eu

Martin Scheicher
European Central Bank, Frankfurt am Main, Germany; email: martin.scheicher@ecb.europa.eu